N O T I C E

THIS DOCUMENT HAS BEEN REPRODUCED FROM MICROFICHE. ALTHOUGH IT IS RECOGNIZED THAT CERTAIN PORTIONS ARE ILLEGIBLE, IT IS BEING RELEASED IN THE INTEREST OF MAKING AVAILABLE AS MUCH INFORMATION AS POSSIBLE

OLD DOMINION UNIVERSITY RESEARCH FOUNDATION

DEPARTMENT OF MECHANICAL ENGINEERING AND MECHANICS
SCHOOL OF ENGINEERING
OLD DOMINION UNIVERSITY
NORFOLK, VIRGINIA

(NASA-CR-164371) THE SULFUR BUDGET OF THE TROPOSPHERE Progress Report, 1 Dec. 1979 - 30 Nov. 1980 (Old Dominion Univ., Norfolk, Va.) 56 p HC A04/MF A01 CSCL 13B
N81-24603
Unclas
G3/45 42511

THE SULFUR BUDGET OF THE TROPOSPHERE

JUN 1981
RECEIVED
NASA STI FACILITY
ACCESS DEPT.

By

S.N. Tiwari, Principal Investigator

and

T.R. Augustsson

Progress Report
For the period December 1, 1979 - November 30, 1980

Prepared for the
National Aeronautics and Space Administration
Langley Research Center
Hampton, Virginia

Under
Cooperative Agreement NCCI-30
Joel S. Levine, Technical Monitor
Atmospheric Environmental Science Division

February 1981

DEPARTMENT OF MECHANICAL ENGINEERING AND MECHANICS
SCHOOL OF ENGINEERING
OLD DOMINION UNIVERSITY
NORFOLK, VIRGINIA

THE SULFUR BUDGET OF THE TROPOSPHERE

By

S.N. Tiwari, Principal Investigator

and

T.R. Augustsson

Progress Report
For the period December 1, 1979 - November 30, 1980

Prepared for the
National Aeronautics and Space Administration
Langley Research Center
Hampton, Virginia 23665

Under
Cooperative Agreement NCCI-30
Joel S. Levine, Technical Monitor
Atmospheric Environmental Science Division

Submitted by the
Old Dominion University Research Foundation
P.O. Box 6369
Norfolk, Virginia 23508

February 1981

FOREWORD

This report summarizes work done under NASA Cooperative Agreement NCCI-30 during the period December 1, 1979 through November 30, 1980. This agreement was supported by NASA/Langley Research Center (LaRC) through the Atmospheric Sciences Branch of the Atmospheric Environmental Science Division. The technical monitor was Dr. Joel S. Levine of the Atmospheric Environmental Science Division.

TABLE OF CONTENTS

	Page
FOREWARD	ii
SUMMARY	1
INTRODUCTION	1
TROPOSPHERIC SULFUR SPECIES	4
Introduction	4
Sulfur Dioxide	6
Carbonyl Sulfide	6
Hydrogen Sulfide	6
Carbon Disulfide	7
Sulfuric Acid	7
Sulfurous Acid Radical	8
Intermediate Sulfur Species	8
ONE-DIMENSIONAL TROPOSPHERIC PHOTOCHEMICAL MODEL	9
RESULTS AND DISCUSSION	19
Introduction	19
Sulfur dioxide	19
Carbonyl sulfide	23
Hydrogen sulfide	25
Carbon disulfide	27
Sulfuric acid	27
Sulfurous acid radical	29
Intermediate sulfur species	31
FUTURE PERTURBATIONS TO THE SULFUR BUDGET	34
APPENDIX A: THE CONTINUITY EQUATION	38
APPENDIX B: NUMERICAL SOLUTION OF THE CONTINUITY EQUATION	40
APPENDIX C: BOUNDARY CONDITIONS	42
APPENDIX D: PHOTODISSOCIATION RATE CALCULATIONS	45
APPENDIX E: CONVERGENCE CRITERIA	47
REFERENCES	48

LIST OF TABLES

Table		Page
1	Photochemical reactions	9
2	Chemical reactions	10

LIST OF FIGURES

Figure		
1	Reaction paths of the sulfur species included in the NASA/LaRC one-dimensional global tropospheric photochemical model	5
2	Calculated vertical profile of SO_2 with and without heterogeneous loss	21
3	Vertical profiles of SO_2 as a function of depositional velocity w	22
4	Calculated vertical profile of carbonyl sulfide (COS)	24
5	Calculated vertical profile of hydrogen sulfide (H_2S)	26
6	Calculated vertical profile of carbon disulfide (CS_2)	28
7	Calculated vertical profile of sulfuric acid (H_2SO_4) and of the sulfurous acid radical (HSO_3)	30
8	Calculated vertical profiles of the intermediate sulfur species.	32
9	Vertical profiles of SO_2 as a function of varying the hydroxyl radical OH	36

THE SULFUR BUDGET OF THE TROPOSPHERE

By

S.N. Tiwari[1] and T.R. Augustsson[2]

SUMMARY

A one-dimensional photochemical tropospheric model has been used to calculate the vertical profiles of tropospheric species. Particular attention is focused on the recent inclusion of the chemistry of the sulfur group, which consists of 13 species involving a total of 45 chemical reactions. It is found that the chemistry of the sulfur species, because it is largely anthropogenic, plays an increasingly important role in the distribution of tropospheric gases. The calculated vertical profiles are compared to available measurements and generally found to be in good agreement.

INTRODUCTION

During the last few years there has been a growing concern over possible anthropogenic effects on the troposphere. The chemistry of the sulfur group is particularly interesting since the emissions of the species in the sulfur family are to a large extent anthropogenic in origin. Of all the tropospheric chemical families, sulfur is perhaps the least studied and understood. Thus, a detailed scheme to calculate the vertical distributions of 13 sulfur gases in the troposphere has been developed. Studies of sulfur in the atmosphere have primarily been concerned with the so-called "aerosol layer" (refs. 1 - 5) or concentrated on highly specific reaction paths and mechanisms in the troposphere (refs. 6 - 7) or certain regions (refs. 8 - 10). Very few global assessments of sulfur species exist (refs. 11 - 12), and those studies are qualitative in nature.

[1] Eminent Professor, Department of Mechanical Engineering and Mechanics, Old Dominion University, Norfolk, Virginia 23508.

[2] Graduate Research Assistant, Department of Mechanical Engineering and Mechanics, Old Dominion University, Norfolk, Virginia 23508.

The recently developed sulfur package allows for quantification (ref. 13).

The research work in this area has been going on for some time, and we now have a one-dimensional, time-independent, global, tropospheric, photochemical model. The model currently includes the chemistry and photochemistry of OH, HO_2, NO_x(= NO + NO_2), HNO_3, NO_3, N_2O_5, HNO_2, CH_3, CH_3O_2, CH_3OOH, CH_3O, H_2CO, HCO, O, O('D), O_3, H, NH, NH_2, NH_3, N_2H_2, N_2H_3, N_2H_4, S, SO, SO_2, SO_3, HSO_3, H_2SO_4, HS, H_2S, CS, CS_2, CH_3SH, CH_3SCH_3, and COS. Of these 36 species, 16 are being transported (i.e., we use the continuity equation) and the remaining 20 are assumed to be in photochemical equilibrium (because they are short lived). There are 108 reactions and 12 photodissociations in the current model, and the vertical transport is simulated by the use of eddy diffusivities. The results of the present model have been compared with results of other models with similar chemistry, rate coefficients, and eddy diffusion parameters. In general, good agreements between various results has been found. Recently, an "ammonia package" has been included in the present model. This consists of the chemistry of NH_3 and five other closely related species. A total of 21 chemical reactions has been added to describe accurately the vertical profiles of the "ammonia group." Ammonia has been the subject of intensive studies, and the results have been reported in references 14 to 17.

The significance of coupled radiative-chemical studies of the Earth's troposphere has been emphasized strongly in the NASA Reference Publication 1022 titled "Man's Impact on the Troposphere" (Lectures in Tropospheric Chemistry, ref. 11). It is evident from this publication that the chemical composition of the troposphere is determined by complex geochemical cycles of carbon, nitrogen, sulfur, oxygen, and hydrogen species between the atmosphere, the oceans, the crust, and the biosphere. In recent years, anthropogenic activities have become a significant source of tropospheric species. As stated in the above reference, changes in the natural abundance of tropospheric species may alter other species via chemistry as well as produce perturbations in climate. For example, tropospheric ozone is strongly affected by tropospheric levels of nitrogen dioxide and methane, and stratospheric ozone is controlled by tropospheric nitrous oxide. Many of these anthropogenically produced species have absorption

lines within the 8- to 12-μm atmospheric window, which contributes to the greenhouse effect. These greenhouse absorbers include carbon dioxide, methane, nitrous oxide, ammonia, and ozone. The information available in the cited reference, therefore, indicates the need for coupled radiative-chemical studies of the Earth's troposphere in a systematic manner.

The coupling between the Naval Research Laboratory's radiative transfer model (which includes Rayleigh and Mie scattering and surface albedo) to the NASA/LaRC one-dimensional tropospheric photochemical model has recently been completed. The preliminary results indicate that the vertical distributions of several key tropospheric species are altered significantly (ref. 18). The next report will address this topic in more detail.

The next section of this report ("Tropospheric Sulfur Species") reviews and summarizes the existing literature on sulfur species. Each sulfur species is discussed briefly and available measurements are identified. The section titled "One-Dimensional Tropospheric Photochemical Model" then discusses the philosophy of modeling as well as the NASA/LaRC one-dimensional global, tropospheric, photochemical model used for the calculations summarized under "Results and Discussion." This model now consists of 37 chemical species (13 of which are in the sulfur group) and 108 reactions (of which 45 are sulfur related). The major text of "Results and Discussion" describes all the reactions, productions, losses and lifetimes for each sulfur species as calculated by the present work. We have found that the sulfur species family consists of gases in various states of oxidation (from highly reduced to highly oxidized) with a wide range of lifetimes (from 10^{-7} s to 4 mo). In the same section we identify the various sources (i.e., natural vs. anthropogenic) and sinks (homogeneous vs. heterogeneous) for all sulfur species. In the concluding section ("Future Perturbations to the Sulfur Budget"), some global implications resulting from perturbations in the sulfur budget are discussed. The continuity equation and its numerical solution together with appropriate boundary conditions are discussed in Appendixes A to C. Appendix D describes the calculations of incident solar radiation and photodissociation rates, while Appendix E discusses the convergence criteria employed in this study.

TROPOSPHERIC SULFUR SPECIES

Introduction

According to R. Stewart et al. (ref. 11, p. 42):

> The abundances, sources and sinks, and photochemistry of atmospheric sulfur compounds are all poorly understood relative to oxygen, carbon or nitrogen compounds. Various sulfur species are important components of air pollution in many parts of the world. The anthropogenic input to the sulfur cycle is clearly significant and likely to increase in magnitude, but the consequences of these facts have been relatively little explored.

They further conclude (p. 46) that:

> Man is also intervening in the sulfur cycle, but global-scale consequences of this influence have yet to be identified. Most of the sulfur dioxide that enters the atmosphere is of industrial origin and can potentially alter such things as the atmospheric aerosol loading and the acidity of rainfall over at least mesoscale regions. The 26 Mt/yr of sulfur added to the soil in fertilizers is relatively large compared with natural sources. If substantially increased coal burning occurs in the future in response to shortages of alternate fuels, the magnitude of the industrial sulfur source will increase still further. It is essential that some attempts to understand the potential impact of this fact be made in future research.

The purpose of this study is to explore and try to understand the implications that an increase in sulfur loading will have on global tropospheric chemistry. It has been known for a long time that species of the sulfur family adversely affect the air quality on the local and regional scales. This is due mainly to anthropogenic emissions in large metropolitan areas. Furthermore, it has been known for about two decades that species of the sulfur family diffuse upward into the stratosphere where they form sulfate particulates that constitute the so-called "aerosol layer" usually found at around 20 km (ref. 2). Natural emissions of particulates from volcanoes also contribute to the aerosol layer.

The sulfur group consists of species in various reduced and oxidized states and with widely varying lifetimes. All sulfur species have in common an unrelenting trend toward further oxidation. The oxidation chain for the sulfur family is shown schematically in figure 1.

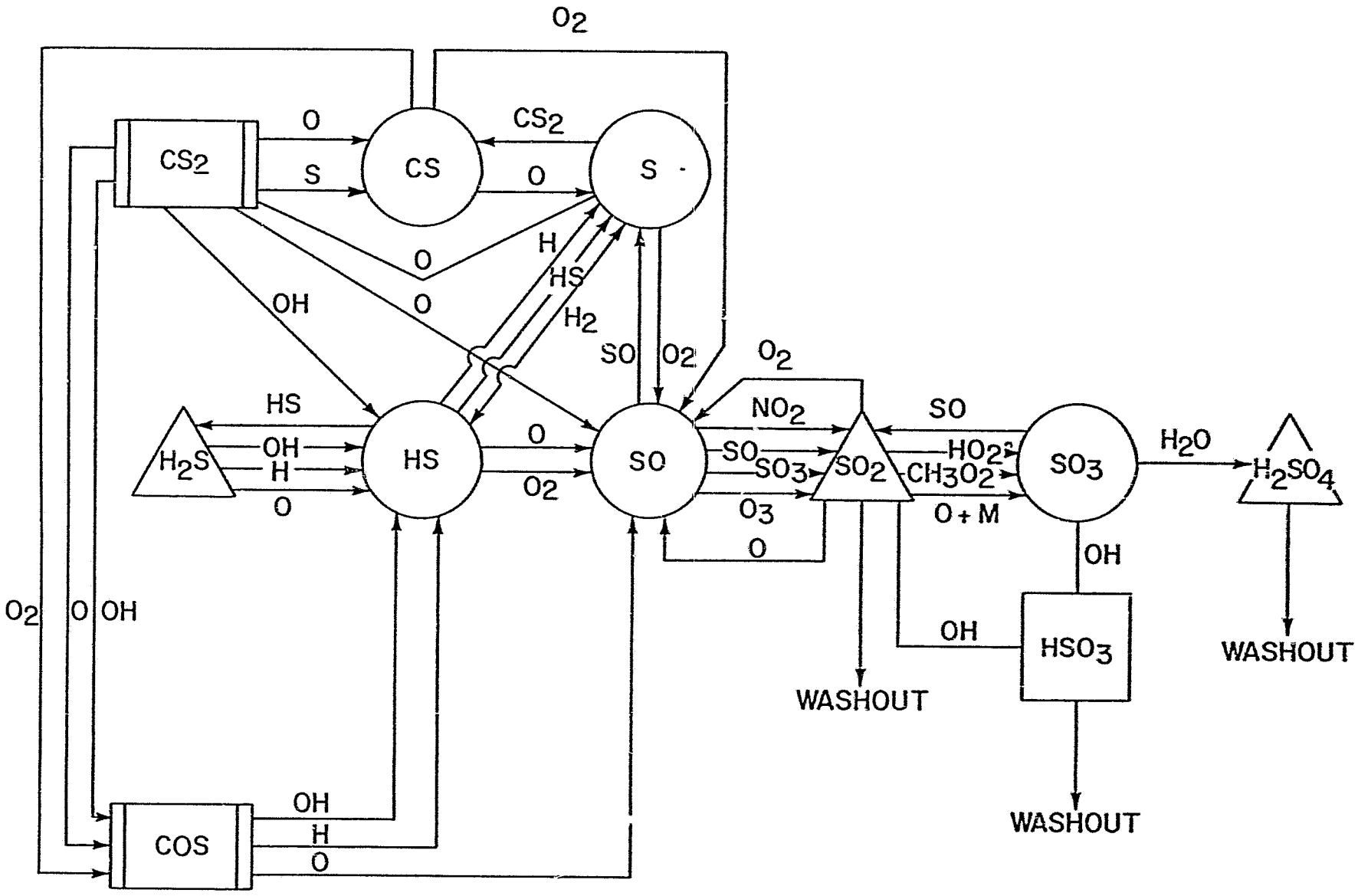

Figure 1. Reaction paths of the sulfur species included in the NASA/LaRC one-dimensional global tropospheric photochemical model.

Sulfur Dioxide (SO_2 — mixing ratio = 5.0×10^{-10})

In large concentrations, SO_2 is very toxic to animals and plants. It is an important precursor to formation of particulates. This affects the aerosol loading, which has climatic implications in addition to the very obvious problem of reduced visibility. Another climatic aspect to consider is the thermal infrared absorption bands that SO_2 has at 8.7 μm and 7.3 μm (ref. 19). At the present time the measurements of SO_2 are very inconclusive and in some cases contradictory. For example, Georgii and Gravenhorst (ref. 20) and Maroulis et al. (ref. 21) found that sulfur dioxide increases with altitude, while Georgii (ref. 22) found a decrease with altitude. This fact is currently a source of some controversy in the scientific literature.

Carbonyl Sulfide (COS — mixing ratio = 5.0×10^{-10})

COS is a very stable molecule and is consequently well mixed in the troposphere. It diffuses into the stratosphere where it is believed to undergo photodissociation. It subsequently recombines with other species to form SO_2, which, in the stratosphere, is believed to be the gaseous precursor of the aerosol layer (refs. 1 - 2). The observational data of COS indicate a relatively uniform distribution. Sandalls and Penkett (ref. 23) found values varying from 4.0×10^{-10} to 5.6×10^{-10} with a mean concentration of 5.1×10^{-10}. Maroulis et al. (ref. 24) measured averaged concentrations of 4.35×10^{-10} in Philadelphia, 4.54×10^{-10} at Wallops Island (Virginia), and 5.11×10^{-10} at Lawton (Oklahoma). Torres et al. (ref. 25) found values ranging from 4 to 5×10^{-10} during the so-called "GAMETAG" flights. The average value during those flights was 4.7×10^{-10}. Hanst et al. (ref. 26) found values of about 2 to 3×10^{-10} in some measurements that had large experimental uncertainties associated with them.

Hydrogen Sulfide (H_2S — mixing ratio = 2.0×10^{-10})

Hydrogen sulfide is formed primarily by microbial activity in the soil and in tidal flats (ref. 27), but it is also emitted by volcanoes (ref. 28) as well as by some industrial activities such as wood pulping (ref. 29) and sewage treatment (ref. 30). Measurements of the vertical distribution are very sparse, but seem to indicate a very rapid decrease with altitude, particularly

in the first few meters (ref. 22). The mixing ratio at the surface has been estimated at 0.2 parts per billion by volume (ppb_v)(ref. 31). The measurements by Georgii (ref. 22) seem to verify this value.

Carbon Disulfide (CS_2 — mixing ratio = 1.9×10^{-10})

CS_2 is formed both naturally by volcanic emissions (ref. 32) and by anthropogenic emissions such as manufacturing of petroleum (ref. 33) and of synthetic fiber (E.P.A., 1973-1975, refs. 34-36). CS_2 has been measured in seawater (ref. 37), giving an almost constant value of 5.2×10^{-13} g/ml of water over a wide range of latitudes. This would indicate a natural source for carbon disulfide. Atmospheric measurements vary from 7×10^{-11} to 3.7×10^{-10} with an average value of 1.9×10^{-10} (ref. 23). It has recently been suggested in references 4 and 6 that the oxidation of CS_2 to form SO_2 might be similar to the oxidation for COS. It has also been argued that CS_2 might oxidize to form COS (ref. 4). In either case, CS_2 is an important precursor for aerosol formation.

Sulfuric Acid (H_2SO_4 — mixing ratio = 1.0×10^{-10})

H_2SO_4 is formed chemically as well as naturally, by volcanic emission (ref. 38), and anthropogenically, in automobiles (ref. 36) and in H_2SO_4 manufacturing (ref. 39). Sulfuric acid occurs both in liquid and solid forms. It forms the solid form (sulfate, SO_4^{2-}) when it recombines with cations other than hydrogen. Hence, H_2SO_4 affects the environment in two ways:

(i) by formation of aerosol particulates, which reduce both incoming radiation and visibility, and

(ii) by lowering the pH in rainwater.

In Scandinavia, which is downwind from the large industrial areas in Germany and Great Britain, a gradual lowering of pH in rainwater has been observed. The average rate of decrease has been 0.3 to 0.4 units per decade (ref. 40). Similar acidic rainfalls have been observed in the Atlantic provinces of Canada, downwind of the highly industrialized metropolitan "northeast corridor" (ref. 9). Acid precipitation is known to have an adverse effect on soils and vegetation. If a soil becomes more acidic, leaching of nutrients in the top soil layer (humus) is accelerated (ref. 7).

This leaching affects, among other things, the rate of growth of trees: for example, forest productivity in Scandinavia has decreased by one percent per year during the last few decades with high incidents of acidic precipitation (ref. 9). Ammonia (NH_3) plays an important role in neutralizing acidic sulfur species. Consequently, if the global sulfur budget increases more rapidly than the global ammonia budget, a further increase in acid precipitation would be expected.

Sulfurous Acid Radical (HSO_3 -- mixing ratio = 1.0×10^{-11})

It is of utmost importance to find out how gaseous sulfur is eventually converted into aerosol particulates. One reaction scheme that eventually produces H_2SO_4 is via the HSO_3 radical. This HSO_3 to H_2SO_4 conversion is not immediate, however. It is therefore of considerable interest to discover the ultimate fate of the HSO_3 radical. Some complex reaction schemes for HSO_3 have been suggested (refs. 41-43), but none is supported by rate constants.

Intermediate Sulfur Species

The five intermediate sulfur species listed below are all very short lived and are therefore assumed to be in photochemical equilibrium (PCE). Their lifetimes vary from 10^{-2} to 10^{-7} seconds and, hence, they react almost instantaneously to form other species. Due to their reactivity they cannot be measured in situ. Their vertical profiles are calculated from known kinetic data.

(i)	Sulfoxy	(SO);	(mixing ratio = 4.0×10^{-17})
(ii)	Carbon sulfide	(CS);	(mixing ratio = 6.0×10^{-20})
(iii)	Thiohydroxyl radical	(HS);	(mixing ratio = 4.0×10^{-21})
(iv)	Sulfur trioxide	(SO_3);	(mixing ratio = 4.0×10^{-22})
(v)	Atomic sulfur	($S(^3p)$);	(mixing ratio = 2.0×10^{-26})

ONE-DIMENSIONAL TROPOSPHERIC PHOTOCHEMICAL MODEL

The one-dimensional, global, tropospheric, photochemical model that has been under development at NASA/LaRC now contains a total of 108 chemical reactions and 12 photolytic reactions. Of this, the recent inlcusion of the sulfur group contributes 45 reactions (reaction 64 to reaction 108). Table 1 lists the photodissociation processes that are included with their rates at the surface for a solar zenith angle of 45°. Table 2 lists all the chemical reactions with appropriate rate coefficients.

Table 1. Photochemical reactions.

Photodissociation No.	Process	Rate (Z=0), s^{-1}(45°)
1	$O_3 + h\nu \rightarrow O(^1D) + O_2$	6.3 E-6
2	$O_3 + h\nu \rightarrow O + O_2$	3.0 E-4
3	$NO_2 + h\nu \rightarrow NO + O$	7.6 E-3
4	$NO_3 + h\nu \rightarrow NO_2 + O$	8.2 E-2
5	$NO_3 + h\nu \rightarrow NO + O_2$	2.0 E-3
6	$N_2O_5 + h\nu \rightarrow NO_2 + NO_3$	2.0 E-5
7	$HNO_3 + h\nu \rightarrow OH + NO_2$	1.6 E-7
8	$HNO_2 + h\nu \rightarrow OH + NO$	4.8 E-4
9	$H_2O_2 + h\nu \rightarrow 2\ OH$	1.6 E-6
10	$CH_2O + h\nu \rightarrow HCO + H$	2.0 E-5
11	$CH_2O + h_2 \rightarrow H_2 + CO$	6.5 E-5
12	$CH_3OOH + h\nu \rightarrow CH_3O + OH$	1.6 E-6

Table 2. Chemical reactions.

Reaction No.	Reaction	Rate Expression (mole — cgs units)	Reference
1	$CH_4 + OH \rightarrow CH_3 + H_2O$	2.4E-12*exp(-1710.0/T)	(a)
2	$CH_4 + O(^1D) \rightarrow CH_3 + OH$	1.3E-10	(a)
3	$CH_3 + O_2 + M \rightarrow CH_3O_2 + M$	$2.2E\text{-}31*(300.0/T)^{2.2}$	(a)
4	$CH_3O_2 + HO_2 \rightarrow CH_3OOH + O_2$	3.0E-11*exp(-500.0/T)	(b)
5	$CH_3OOH + OH \rightarrow CH_3O_2 + H_2O$	6.2E-12*exp(-750.0/T)	(a)
6	$CH_3O_2 + NO \rightarrow CH_2O + HNO_2$	0.0	(c)
7	$CH_3O_2 + NO_2 \rightarrow CH_2O + HNO_3$	0.0	(d)
8	$CH_3O_2 + NO \rightarrow CH_3O + NO_2$	8.0E-12	(a)
9	$CH_3O + O_2 \rightarrow CH_2O + HO_2$	5.0E-13*exp(-2000.0/T)	(a)
10	$CH_2O + OH \rightarrow HCO + H_2O$	1.7E-11*exp(-100.0/T)	(a)
11	$HCO + O_2 \rightarrow CO + HO_2$	5.0E-12	(a)
12	$CO + OH \rightarrow CO_2 + H$	$1.35E\text{-}13*(1 + P_{atm})$	(a)
13	$CO + HO_2 \rightarrow CO_2 + OH$	1.0E-20	(e)
14	$H_2 + OH \rightarrow H + H_2O$	1.2E-11*exp(-2200.0/T)	(a)
15	$H + O_2 + M \rightarrow HO_2 + M$	$5.5E\text{-}32*(300.0/T)^{1.4}$	(a)
16	$O(^1D) + H_2O \rightarrow 2\ OH$	2.3E-10	(a)
17	$O(^1D) + H_2 \rightarrow H + OH$	9.9E-11	(a)
18	$HO_2 + OH \rightarrow H_2O + O_2$	4.0E-11	(a)
19	$OH + OH \rightarrow H_2O + O$	1.0E-11*exp(-500.0/T)	(a)
20	$HO_2 + HO_2 \rightarrow H_2O_2 + O_2$	2.5E-12	(a)
21	$H_2O_2 + OH \rightarrow HO_2 + H_2O$	1.0E-11*exp(-750.0/T)	(a)
22	$HO_2 + NO \rightarrow OH + NO_2$	3.4E-12*exp(250.0/T)	(a)
23	$HO_2 + NO_2 \rightarrow HNO_2 + O_2$	3.0E-14	(f)

Table 2. (continued).

Reaction No.	Reaction	Rate Expression (mole — cgs units)	Reference
24	$OH + NO_2 \xrightarrow{M} HNO_3$	$2.6E\text{-}30*(300/T)^{2.9}$	(a)
25	$OH + NO \xrightarrow{M} HNO_2$	2.0E-12	(g)
26	$HNO_3 + OH \rightarrow NO_3 + H_2O$	8.5E-14	(a)
27	$HNO_3 \rightarrow$ rainout	1.0E-6	(d)
28	$NO_2 + O_3 \rightarrow NO_3 + O_2$	1.2E-13*exp(2450.0/T)	(a)
29	$NO + O_3 \rightarrow NO_2 + O_2$	2.3E-12*exp(-1450.0/T)	(a)
30	$NO_3 + NO_2 \xrightarrow{M} N_2O_5$	3.8E-12	(g)
31	$NO_3 + NO_2 \rightarrow NO + NO_2 + O_2$	2.3E-13*exp(-1000.0/T)	(h)
32	$NO_3 + NO \rightarrow 2\ NO_2$	8.7E-12	(i)
33	$NO + NO_2 + H_2O \rightarrow 2\ HNO_2$	6.0E-37	(j)
34	$N_2O_5 + H_2O \rightarrow 2\ HNO_3$	1.0E-20	(k)
35	$N_2O_5 \rightarrow NO_3 + NO_2$	5.7E-14*exp(-10600.0/T)	(g)
36	$O + O_2 + M \rightarrow O_3 + M$	$6.2E\text{-}34*(300.0/T)^{2.1}$	(a)
37	$O(^1D) + M \rightarrow O + M$	3.2E-11	(l)
38	$OH + O_3 \rightarrow HO_2 + O_2$	1.6E-12*exp(-940.0/T)	(a)
39	$HO_2 + O_3 \rightarrow OH + 2\ O_2$	1.1E-14*exp(-580.0/T)	(a)
40	$OH + HNO_2 \rightarrow NO_2 + H_2O$	2.1E-12	(m)
41	$O(^1D) + CH_4 \rightarrow CH_2O + H_2$	1.4E-11	(a)
42	$N_2H_4 + H \rightarrow N_2H_3 + H_2$	9.9E-12*exp(-1200.0/T)	(n)
43	$N_2H_3 + N_2H_3 \rightarrow 2\ NH_3 + N_2$	$K_{43} << K_{44}$	(o)
44	$N_2H_3 + N_2H_3 \rightarrow N_2H_4 + N_2H_2$	6.0E-11	(o)
45	$N_2H_3 + H \rightarrow 2\ NH_2$	2.7E-12	(o)
46	$NH_3 + O \rightarrow NH_2 + OH$	6.6E-12*exp(-3300.0/T)	(n)

Table 2. (continued).

Reaction No.	Reaction	Rate Expression (mole — cgs units)	Reference
47	$NH_3 + O(^1D) \rightarrow NH_2 + OH$	2.5E-10	(a)
48	$NH_3 + OH \rightarrow NH_2 + H_2O$	2.3E-12*exp(-800.0/T)	(n)
49	$NH_3 + H \rightarrow NH_2 + H_2$	1.0E-16	(n)
50	$NH_2 + O \rightarrow HNO + H$	1.8E-12	(n)
51	$NH_2 + O \rightarrow NH + OH$	1.8E-12	(n)
52	$NH_2 + OH \rightarrow NH_3 + O$	1.0E-13	(n)
53	$NH_2 + H_2 \rightarrow NH_3 + H$	1.0E-16	(n)
54	$NH_2 + NO \rightarrow N_2 + H_2O$	2.1E-11	(n)
55	$NH_2 + NH_2 \rightarrow N_2H_4$	1.0E-10	(o)
56	$NH + NO \rightarrow N_2 + O + H$	4.7E-11	(n)
57	$NH + O_2 \rightarrow NO + OH$	6.0E-13	(p)
58	$NH + NO \rightarrow N_2 + OH$	3.9E-11	(q)
59	$HNO + O_2 \rightarrow NO + HO_2$	2.1E-20	(n)
60	$HNO + M \rightarrow NO + H + M$	5.0E-08*exp(-24500.0/T)	(n)
61	$HNO + H \rightarrow NO + H_2$	5.0E-14	(n)
62	$HNO + HNO \rightarrow N_2O + H_2O$	4.0E-15	(n)
63	$H + H + M \rightarrow H_2 + M$	8.3E-33	(n)
64	$H_2S + OH \rightarrow HS + H_2O$	1.05E-11*exp(-200.0/T)	(a)
65	$HS + O \rightarrow SO + H$	1.6E-10	(n)
66	$HS + O_2 \rightarrow SO + OH$	1.0E-13	(n)
67	$HS + NO \rightarrow$ products	1.0E-12	(r)
68	$SO + O_2 \rightarrow SO_2 + O$	7.5E-13*exp(-3250.0/T)	(n)
69	$SO + NO_2 \rightarrow SO_2 + NO$	1.5E-11	(s)
70	$CS_2 + O \rightarrow SO + CS$	3.1E-11*exp(-640.0/T)(f_{70} = 0.8)	(a)

Table 2. (continued).

Reaction No.	Reaction	Rate Expression (mole — cgs units)	Reference
71	$CS_2 + O \rightarrow S + COS$	3.1E-11*exp(-640.0/T)(f_{71} = 0.1)	(a)
72	$CS_2 + O \rightarrow S_2 + CO$	3.1E-11*exp(-640.0/T)(f_{72} = 0.1)	(a)
73	$CS + O \rightarrow S + CO$	2.2E-11	(n)
74	$CS + O_2 \rightarrow SO + CO$	<3.0E-18	(s)
75	$CS + O_2 \rightarrow COS + O$	<3.0E-18	(s)
76	$S + O_2 \rightarrow SO + O$	2.2E-12	(t)
77	$SO_2 + OH(+M) \rightarrow HSO_3(+M)$	(8.2E-13*M)/(7.9E17 + M)	(u)
78	$SO_2 + HO_2 \rightarrow SO_3 + OH$	2.0E-17	(v)
79	$SO_2 + CH_3O_2 \rightarrow SO_3 + CH_3O$	<3.3E-15	(w)
80	$SO_3 + H_2O \rightarrow H_2SO_4$	9.1E-13	(n)
81	$SO_2 + O \rightarrow SO + O_2$	(2.1E-10/$_T$0.5)*exp(-9980.0/T)	(n)
82	$HS + H \rightarrow S + H_2$	2.5E-11	(n)
83	$S + H_2 \rightarrow HS + H$	2.2E-25	(n)
84	$H_2S + H \rightarrow HS + H_2$	1.29E-11*exp(860.0/T)	(n)
85	$COS + H \rightarrow HS + CO$	2.2E-14	(n)
86	$COS + OH \rightarrow HS + CO_2$	5.7E-14	(a)
87	$CS_2 + OH \quad HS + COS$	1.9E-13	(a)
88	$S + CS_2 \rightarrow S_2 + CS$	6.5E-13	(n)
89	$S + COS \rightarrow S_2 + CO$	2.8E-12*exp(-2050.0/T)	(n)
90	$SO + SO \rightarrow S + SO_2$	3.0E-15	(n)
91	$SO + SO_3 \rightarrow 2\ SO_2$	2.0E-15	(n)
92	$SO_2 + CH_3(+M) \rightarrow CH_3SO_2(+M)$	3.0E-13	(n)
93	$HS + HS \rightarrow H_2S + S$	1.2E-11	(n)
94	$CH_3SH + O \rightarrow CH_3 + HSO$	1.9E-12	(x)

Table 2. (concluded).

Reaction No.	Reaction	Rate Expression (mole — cgs units)	Reference
95	$CH_3SH + O \rightarrow CH_3SO + H$	1.9E-12	(x)
96	$CH_3SH + O \rightarrow CH_3SOH$	1.9E-12	(x)
97	$CH_3SH + OH \rightarrow$ products	3.4E-11	(y)
98	$CH_3SCH_3 + O \rightarrow CH_3SO + CH_3$	4.8E-11	(z)
99	$CH_3SCH_3 + O \rightarrow CH_2S + CH_3O$	6.3E-11	(x)
100	$CH_3SCH_3 + OH \rightarrow$ products	6.08E-12*exp(134.0/T)	(aa)
101	$COS + O \rightarrow SO + CO$	2.1E-11*exp(-2200.0/T)	(a)
102	$H_2O + O \rightarrow HS + OH$	2.4E-12*exp(-1300.0/T)	(a)
103	$SO + O_3 \rightarrow SO_2 + O_2$	2.5E-12*exp(-1050.0/T)	(n)
104	$SO_2 + O + M \rightarrow SO_3 + M$	3.4E-32*exp(-1130.0/T)	(n)
105	$HSO_3 + OH \rightarrow SO_3 + H_2O$	1.0E-11	(bb)
106	$SO_2 \rightarrow$ washout	3.8E-6*(10-Z)/10	(bb)
107	$HSO_3 \rightarrow$ washout	2.3E-5*(10-Z)/10	(bb)
108	$H_2SO_4 \rightarrow$ washout	2.3E-5*(10-Z)/10	(bb)

References:

(a) Chemical Kinetic and Photochemical Data for Use in Stratospheric Modeling, Evaluation Number 2, JPL Publication 79-27, (available from NASA).

(b) Levy, H.: Photochemistry of Minor Constituents in the Troposphere, Planet. Space Sci., Vol. 21, 1973, pp. 575-591.

(c) Pate, C.T.; Finlayson, B.J.; and Pitts, J.N., Jr.: A Long Path Infrared Spectroscopic Study of the Reaction of Methyl-peroxy Free Radicals with Nitric Oxide. J. Amer. Chem. Soc., Vol. 96, 1974, pp. 6554-6558.

(d) Chameides, W.L.; and Stedman, D.H.: Tropospheric Ozone: Coupling Transport and Photochemistry. J. Geophys. Res., Vol. 82, 1977, pp. 1787-1794.

(e) Davis. D.D.; Payne, W.A.; and Stief, L.J.: The Hydro-peroxyl Radical in Atmospheric Chemical Dynamics: Reaction with Carbon Monoxide. Science, Vol. 179, 1973, pp. 280-282.

(f) Hampson, R.F.; and Garvin, D. (eds.): Chemical Kinetics and Photochemical Data for Modelling Atmospheric Chemistry. NBS Tech. Note 866, Nat'l. Bur. of Stand. (Gaithersburg, Md.), 1975, 113 pp.

(g) Baulch, D.L.; Drysdale, D.D.; Horne, D.G.; and Lloyd, A.C.: Evaluated Kinetic Data for High Temperature Reactions. Homogeneous Gas Phase Reactions of the H_2 - N_2 - O_2 System, Vol. 2, Chemical Rubber Company Press (Cleveland, Ohio), 1973.

(h) Garvin, D.; and Hampson, R.F. (eds.): Chemical Kinetics Data Survey 7, Tables of Rate and Photochemical Data for Modelling of the Stratosphere. Rep. NBSIR 74-430, Nat'l. Bur. of Stand. (Gaithersburg, Md.), 1974, 101 pp.

(i) Harker, A.B.; and Johnston, H.S.: Photolysis of Nitrogen Dioxide to Produce Transient O, NO_3, and N_2O_5. J. Phys. Chem., Vol 77, 1973, pp. 1153-1156.

(j) Chan, W.H.; Nordstrum, R.J.; Calvert, J.G.; and Shaw, J.H.: An IRFTS Spectroscopic Study of the Kinetics and the Mechanism of the Reactions in the Gaseous System HONO, HO, HO_2, H_2O. Chem. Phys. Lett., Vol. 37, 1976, pp. 441-446.

(k) Morris, E.D., Jr.; and Niki, H.: Mass Spectrometric Study of the Hydroxyl Radical with Formaldehyde. J. Chem. Phys., Vol. 55, 1971, pp. 1991-1992.

(l) Davidson, J.A.; Sadlowski, C.M.; Schiff, H.I.; Streit, G.E.; Howard, C.J.; Jennings, D.A.; and Schmeltekopf, A.L.: Absolute Rate Constant Determinations for the Deactivation of $O(^1D)$ by Time Resolved Decay of $O(^1D) \rightarrow O(^3p)$ Emission. J. Chem. Phys., Vol. 64, 1976, pp. 57-62.

(m) Cox, R.A.: The Photolysis of Gaseous Nitrous Acid — A Technique for Obtaining Kinetic Data on Atmospheric Photo-oxidation Reactions. In: Proceedings of the Symposium on Chemical Kinetics Data for the Lower and Upper Atmosphere, S.W. Benson ed., Wiley-Interscience (N.Y.), 1975, pp. 379-398.

(n) Hampson, R.F.; and Garvin, D.: Reaction Rate and Photochemical Data for Atmospheric Chemistry - 1977. Nat'l. Bur. of Stand. Special Publication 513, U.S. Government Printing Office (Washington, D.C.), 1978, 111 pp.

(o) Atreya, S.K.; Donahue, T.M.; and Kuhn, W.R.: The Distribution of Ammonia and Its Photochemical Products on Jupiter. Icarus, Vol. 31, 1977, pp. 348-355.

(p) McConnell, J.C.: Atmospheric Ammonia. J. Geophys. Res., Vol 78, 1973, pp. 7812-7821.

(q) Gordon, S.; Mulac, W.; and Nangia, P.: Pulse Radiolysis of Ammonia Gas, 2, Rate of Disappearance of the $NH_2(X^2B_1)$ Radical. J. Phys. Chem., Vol. 75, 1971, pp. 2087-2093.

(r) Bradley, J.N. et al.: Electron Spin Resonance Study of the Reaction of Hydrogen Atoms with Hydrogen Sulfide. J. Chem. Soc. Faraday Trans. I, Vol. 69, 1973, pp. 416-425.

(s) Schofield, K.: Evaluated Chemical Kinetic Rate Constants for Various Gas Phase Reactions. J. Phys. Chem. Ref. Data, Vol. 2, 1973, pp. 25-84.

(t) Davis, D.D.; Klemm, R.B.; and Pilling M.: A Flash Photolysis-Resonance Fluorescence Kinetics Study of Ground-State Sulfur Atoms, I, Absolute Rate Parameters for Reaction of $S(^3P)$ with $O_2(^3\Sigma)$. Int. J. Chem. Kinet., Vol 4, 1972, pp. 367-382.

(u) Moortgat, C.K.; and Junge, C.E.: Pageoph, Vol. 115, 1977, p. 759.

(v) Burrows, J.P.; Cliff, D.I.; Harris, G.W.; Thrush, B.A.; and Wilkinson, J.P.T.: W.M.O. Tech. Note No. 511, 1978, pp. 25-28.

(w) Whitbeck, M.R. et al.: A Kinetic Study of CH_3O_2 and $(CH_3)_3\ CO_2$ Radical Reactions by Kinetic Flash Spectroscopy. Paper presented at 12th Informal Conference on Photochemistry, Nat'l. Bur. of Stand. (Gaithersburg, Md.), June 28, 1976.

(x) Slagle, I.R.; Graham, R.E.; and Gutman, D.: Direct Identification of Reactive Routes and Measurement of Rate Constants in the Reactions of Oxygen Atoms with Methanethiol, Ethanethiol, and Methylsulfide. Int. J. Chem. Kinet., Vol. 8, 1976, pp. 451-458.

(y) Atkinson, R.; Perry, R.A.; and Pitts, J.N., Jr.: Rate Constants for the Reactions of the OH Radical with CH_3SH and CH_3NH_2 over the Temperature Range 299-426°K. J. Chem. Phys., Vol. 66, 1977, pp. 1578-1581.

(z) Lee, J.H.; Timmons, R.B.; and Stief, L.J.: Absolute Rate Parameters for the Reaction of Ground State Atomic Oxygen with Dimethyl Sulfide and Episulfide. J. Chem. Phys., Vol. 64, 1976, pp. 300-305.

(aa) Kurylo, M.J.: Chem. Phys. Lett., Vol. 58, 1978, pp. 233-237.

(bb) Turco, R.P.; Hamill, P.; Toon, O.B.; Whitten, R.C.; and Kiang, C.S.: A One-Dimensional Model Describing Aerosol Formation and Evolution in the Stratosphere: I. Physical Processes and Mathematical Analogs. J. Atmos. Sci., Vol. 36, 1979, pp. 699-717.

Depending on the lifetime of a species, it can either be considered in photochemical equilibrium (PCE) or it will have to undergo transport. The rapidly reacting species have their vertical profiles determined by chemistry alone, while the vertical profiles of the more long-lived species are determined by the combined effects of chemistry and eddy transport, utilizing a time-independent (sometimes called steady-state) continuity equation. The details of the continuity equation are described in Appendix A. Numerically, the continuity equation is solved using a finite-difference form known as the central difference scheme (see Appendix B for a discussion of this). The boundary conditions for the continuity equation can be either a specified number density or a specified flux, as detailed in Appendix C. With the recent inclusion of the sulfur group, the model now contains a total of 37 chemical species. Of this amount, 17 are calculated using the continuity equation: nitric oxide (NO), nitrogen dioxide (NO_2), ozone (O_3), nitric acid (HNO_3), methylhydroperoxy (CH_3OOH), ammonia (NH_3), hydrazine (N_2H_4), two hydrazine derivatives (N_2H_3) and (N_2H_2), hydrogen sulfide (H_2S), sulfur dioxide (SO_2), carbon disulfide (CS_2). carbonyl sulfide (COS), dimethyl sulfide (CH_3SCH_3), methanethiol (CH_3SH), sulfuric acid (H_2SO_4) and sulfurous acid radical (HSO_3). For the rapidly reacting species the condition of PCE is imposed. This includes the following species: the hydroxyl radical (OH), hydroperoxyl radical (HO_2), nitrogen trioxide (NO_3), dinitrogen pentroxide (N_2O_5), nitrous acid (NHO_2), the amino radicals (NH_2 and NH), methylperoxy radical (CH_3O_2), methoxy radical (CH_3O), formaldehyde (H_2CO), formyl radical (HCO), atomic oxygen ($O(^3p)$), the excited oxygen atom ($O(^1D)$), atomic hydrogen (H), nitroxyl radical (HNO), thiohydroxyl radical (HS), sulfoxy radical (SO), sulfur trioxide (SO_3), atomic sulfur ($S(^3p)$) and carbon sulfide (CS). Certain very long-lived and well-mixed atmospheric species are specified as input parameters. This group includes molecular oxygen (O_2), molecular hydrogen (H_2), carbon dioxide (CO_2), carbon monoxide (CO), methane (CH_4), water vapor (H_2O), and hydrogen peroxide (H_2O_2). Nine species are photodisassociated in 12 different paths in the troposphere in addition to participating in chemical reactions: they are ozone (O_3) (2 photolysis paths), nitrogen dioxide (NO_2), nitrogen trioxide (NO_3) (2 photolysis paths), dinitrogen pentoxide (N_2O_5), nitric acid (HNO_3), nitrous acid

(HNO_2), hydrogen peroxide (H_2O_2), methylhydroperoxy (CH_3OOH) and formaldehyde (CH_2O) (2 photolysis paths). The details of the photodissociation calculations are given in Appendix D. In order to ensure internal self-consistency, a convergence criterion is imposed. This criterion is met when there is agreement between two successive runs up to the sixth decimal place. A further description of the convergence condition follows in Appendix E.

Most atmospheric chemistry studies are performed with one-dimensional (vertical) models, whereas two- and three-dimensional models are usually used for studies of atmospheric flow, dynamics and circulation. Since atmospheric chemistry is initiated by photodissociation of various molecules, the vertical coordinate is the important one in atmospheric chemistry studies. One-dimensional models are known as globally averaged models, because all parameters in these models should ideally be globally averaged. Two-dimensional models, or zonally averaged models, employ an averaging technique whereby parameters are averaged according to latitudinal bands, usually on the order of 5° to 10°. These models are mostly used to study certain flow phenomena of zonal character. Two-dimensional models are usually formulated from a phenomenological point of view rather than from first principles. The eddy mixing is usually developed using mixing length theory. Hence, despite increasing the model by one more dimension, the transport coupling is still unsatisfactory since it relies on the choice of eddy coefficients. Three-dimensional models have been under development during the last decade but have yet to be used very extensively due to their nearly prohibitive cost. The three-dimensional models in existence today have mostly been used for dynamic studies. The most sophisticated three-dimensional model in existance uses a mere nine chemical reactions and seven chemical species. It has been calculated that, for each time seven new species are included, the computational cost rises an order of magnitude. Also, the largest digital computers available still do not have adequate storage to fully describe vertical transport. Hence, three-dimensional models must still rely on parameterized vertical eddy diffusivities, a fact that is not fully appreciated even in the scientific community. In one-dimensional models, a lot of storage is available to incorporate vast amounts of chemistry, which have most of their interesting features in the vertical dimension. Furthermore, most chemical interactions are more easily studied with one-dimensional models.

RESULTS AND DISCUSSION

Introduction

In this section the sources and sinks of the sulfur compounds are examined. Some sulfur species are produced chemically as well as emitted anthropogenically. Loss mechanisms include chemical reactions and heterogeneous losses, i.e., rainout, washout, and dry deposition. The chemical production and loss terms for each species listed below are arranged in order of importance.

Sulfur Dioxide (SO_2)

Chemical production.— The chemical production of SO_2 always involves SO (reactions 68, 69, 103, 90, and 91). Of these reactions, only the recombination of sulfoxy with molecular oxygen, O_2, (reaction 68) and sulfoxy with nitrogen dioxide, NO_2, (reaction 69) are of major importance. SO reacting with ozone, O_3, (reaction 103) is of minor importance, while the reactions of SO with itself (reaction 90) and with sulfur trioxide, SO_3, (reaction 91) are negligible.

Chemical loss.— The most important gas phase loss is due to the reaction with the hydroxyl radical, OH, (reaction 77). A minor loss mechanism is due to reaction with the methylperoxy radical, CH_3O_2 (reaction 79). Reactions with the hydroperoxy radical, HO_2, (reaction 78); atomic oxygen, O, in the presence of a third body (reaction 104); the methyl radical, CH_3, (reaction 92); and with atomic oxygen, O, (reaction 81) are all negligible. The lifetime of SO_2 based solely on gas phase chemistry is about 2.5 days.

Anthropogenic emission.— SO_2 is known as a product of fuel combustion (ref. 34). It has also been detected in the exhaust of turbines (ref. 44) and of diesel engines (ref. 36). The application of certain types of fertilizers also emits SO_2 (ref. 10).

Natural emission.— Sulfur dioxide has been found in the smoke from erupting volcanoes (refs. 32, 38).

Heterogeneous loss.— The heterogeneous loss of SO_2 has been estimated to be about 50 percent of the total loss, and is modeled similarly to that

by Turco (ref. 5), with the exception that the NASA/LaRC model has the tropopause at 10 km while the model of Turco uses 13 km for tropopause altitude. Inclusion of the heterogeneous loss of SO_2 lowers its lifetime to slightly less than two days. At the lower boundary, a flux of 1.275×10^{10} molecules cm^{-2} s^{-1} was used together with a depositional velocity of 1.0 cm s^{-1}. This results in a surface mixing ratio of 0.5 ppb. The resulting vertical profile is shown in figure 2. The solid line represents the standard profile while the dashed line is for the case without heterogeneous loss. In both cases a zero flux condition was imposed at the upper boundary. Vertical profiles have been measured by Jost (ref. 45) and by Georgii (ref. 22). In general, these measurements show a decreasing mixing ratio with altitude similar to the calculations with the NASA/LaRC model. One notable exception is a profile by Georgii (ref. 22) over the Atlantic Ocean (dotted line). In this case there is an increase in mixing ratio with altitude. This is consistent with the theory that the oceans act as a sink for SO_2 (ref. 20). Also included are some measurements by Maroulis (ref. 24) and by Jaeschke et al. (ref. 46). The surface mixing ratio of the vertical profiles by Georgii (ref. 22) and Jost (ref. 45) is about an order of magnitude higher than those calculated by the NASA/LaRC model. This is not very surprising, since Georgii's and Jost's measurements were made over western Europe, an area which is known to have a high background concentration of SO_2. Depositional velocities at the surface have a range of 0.1 to 2.5 cm s^{-1} (ref. 47). A value of 1.0 cm s^{-1} has been suggested as an average depositional velocity (ref. 48). The resulting vertical profiles due to different values of the depositional velocity are shown in figure 3. With a slow depositional velocity, a very rapid increase in mixing ratio with altitude results, and conversely with a high depositional velocity the mixing ratio increases slowly with altitude. In all calculations, the downward flux of SO_2 was kept constant at 1.275×10^{10} molecules cm^{-2} s^{-1}. There are numerous estimates of global SO_2 emission. For example, Katz (ref. 49) estimated that 77 Mt were emitted. Subsequent estimates by Robinson and Robbins (ref. 31) indicate that the annual global SO_2 emission is 146 Mt. Of this amount, 70 percent comes from coal combustion, 16 percent from petroleum fuel combustion, and the rest from various processes such as petroleum refining and smelting. Approximately 95 percent of all the anthropogenically emitted sulfur compounds are in the form of SO_2 (ref. 12).

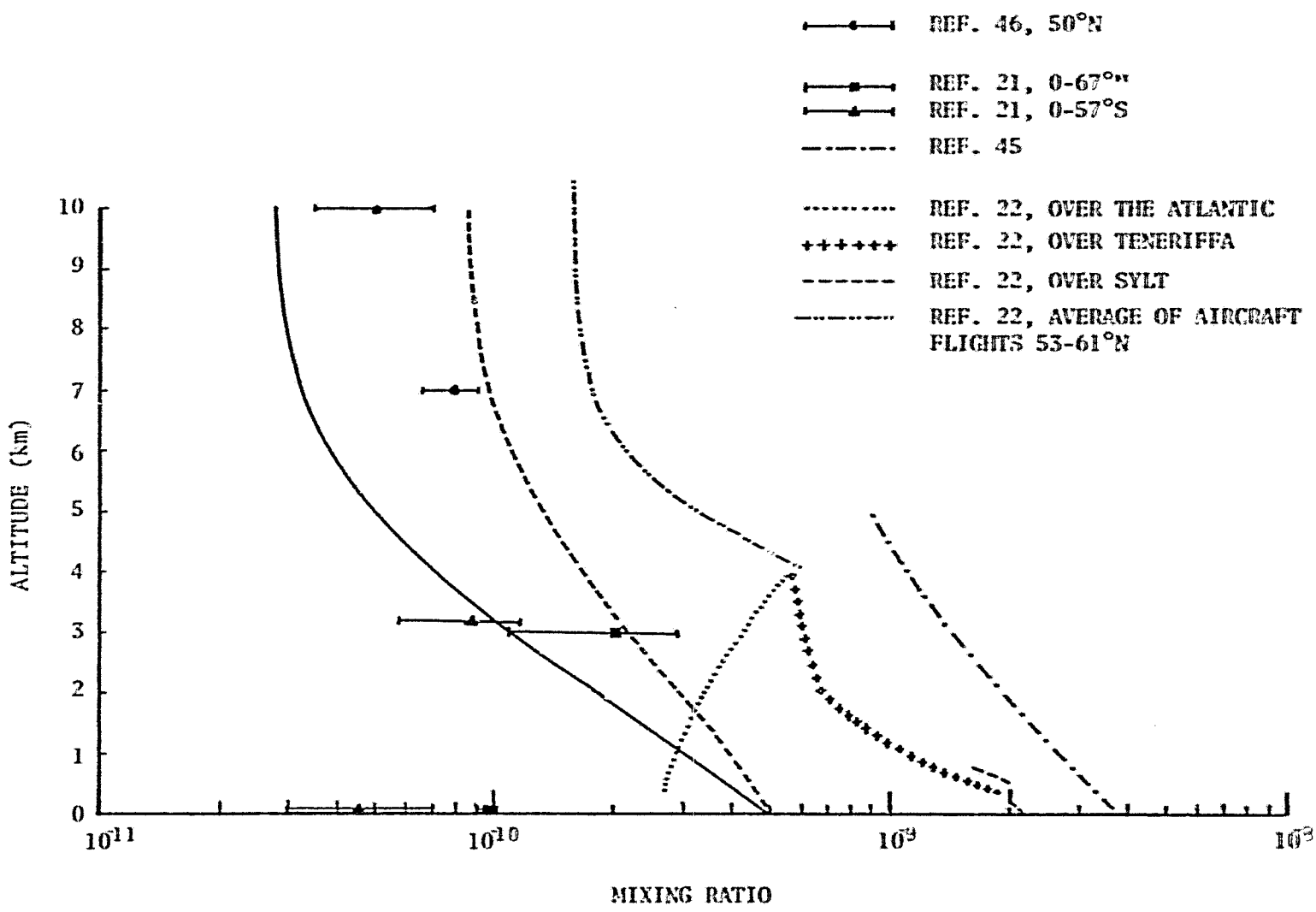

Figure 2. Calculated vertical profile of SO_2 with (solid line) and without (dashed line) heterogeneous loss.

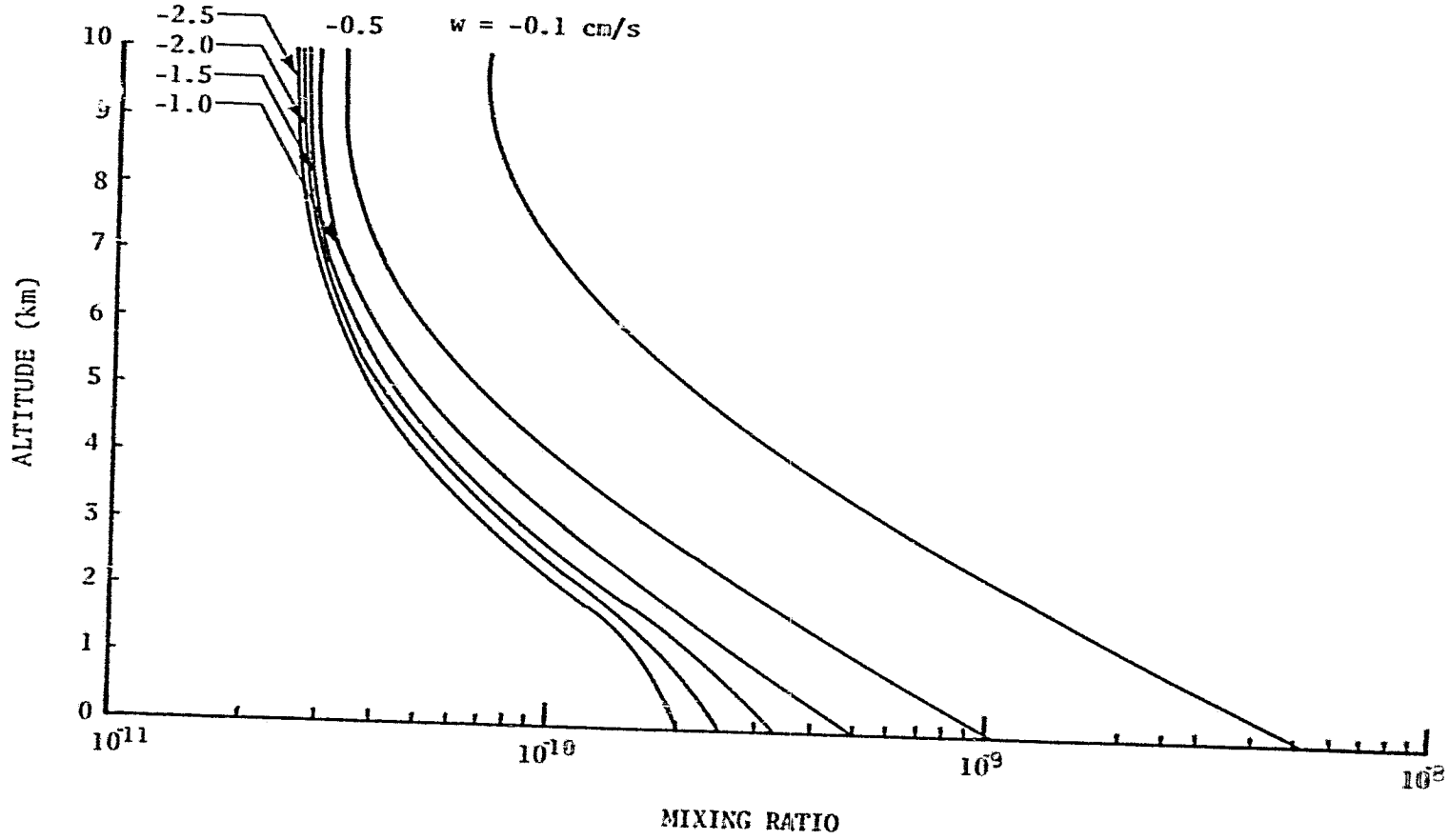

Figure 3. Vertical profiles of SO_2 as a function of depositional velocity w.

A recent estimate of global land sulfur dioxide emission was made by Shinn and Lynn (ref. 10). They estimate anthropogenic emissions to be 183 Mt; 33 Mt of that amount is in the form of fertilizers. Natural emmissions (biogenic and volcanic) account for 21 Mt of sulfur dioxide. Hence, man's activities account for nearly 50 percent of all sulfur dioxide that is emitted into the atmosphere. Since the bulk of this figure involves coal combustion, a switch to greater use of coal as recently suggested is likely to rapidly increase man's contribution to the total sulfur budget.

Carbonyl Sulfide (COS)

Chemical production.— The chemical sources of COS are the reactions of carbon disulfide, CS_2, with the hydroxyl radical, OH, (reaction 87), the reaction of molecular oxygen, O , with carbon sulfide, CS, (reaction 72) and the reaction of molecular oxygen, O, with carbon disulfide (reaction 71). Only reaction 87 is of major importance. Reactions 72 and 71 are only minor pathways for production of COS.

Chemical loss.— The loss mechanisms of carbonyl sulfide are totally dominated by the reaction of COS to OH (reaction 86). All other chemical losses of COS, i.e., reaction with atomic oxygen (reaction 101), reaction with atomic hydrogen, H, (reaction 85) and reaction with atomic sulfur, $S(^3p)$, (reaction 89) can be neglected. The calculated lifetime of COS based on the loss mechanisms mentioned above is about four months. This value agrees reasonably well with a value of 0.6 year reported by Sze and Ko (ref. 4) and 200 days estimated by Logan et al. (ref. 6).

Anthropogenic emission.— COS, which is a very stable molecule, is formed by manmade processes, such as manufacturing of petroleum (ref. 33) and of synthetic fiber (ref. 50).

Natural emission.— Some of the natural processes emitting COS include erupting volcanoes (ref. 32) and forest fires (ref. 51).

In the model calculations, a surface boundary value of 0.5 ppb was used together with a condition of zero flux at the tropopause. The resulting vertical profile is shown in figure 4. The measurements of COS have all been at the surface and indicate that carbonyl sulfide is very well mixed. Sandalls and Penkett (ref. 23)

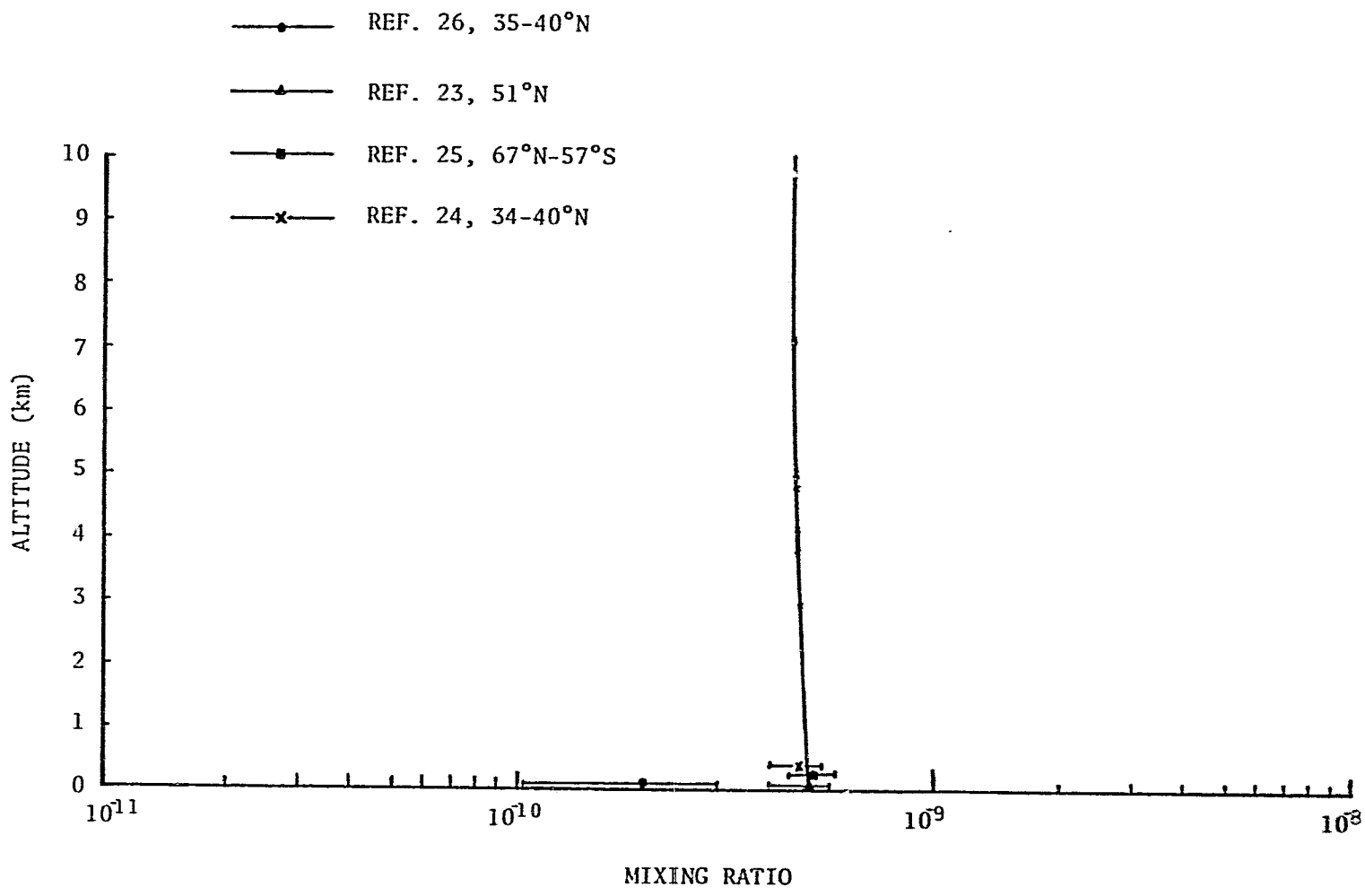

Figure 4. Calculated vertical profile of carbonyl sulfide (COS).

obtained a value of 0.51 ppb. Torres et al. (ref. 25) measured an average value of 0.512 ppb over a wide range of latitudes, while Maroulis et al. (ref. 24) found an average value of 0.467 ppb over 3 different locations in the United States. Some early data by Hanst et al. (ref. 26) indicate a value of 0.2 ppb at the surface, but this measurement was associated with large experimental uncertainties. The vertical profile calculated by the model shows a nearly constant mixing ratio in the troposphere as would be expected from its long lifetime. COS diffuses into the stratosphere, where it undergoes photolysis forming SO (ref. 1). Hence, COS would be an important precursor to the formation of the particulates that constitute the aerosol layer.

Hydrogen Sulfide (H_2S)

Chemical production.— The only known chemical production of H_2S in the atmosphere is due to the reaction of the thiohydroxyl radical, HS, with itself (reaction 93). This is only of very minor importance.

Chemical loss.— The primary loss mechanism for hydrogen sulfide is the reaction of H_2S to OH (reaction 64). The losses due to reactions with atomic oxygen (reaction 102) and with atomic hydrogen (reaction 84) are negligible. The calculated lifetime of H_2S based on these three chemical losses is a little more than one day.

Anthropogenic emission.— Some of the industrial activities that have been identified as emitting H_2S include wood pulping (ref. 29) and sewage treatment (ref. 30).

Natural emission.— H_2S is formed primarily by microbial activity (ref. 27). Volcanoes also emit hydrogen sulfide (ref. 28) as does animal waste (ref. 8).

The only measurements available for H_2S are those of Georgii (ref. 22) and of Slatt et al. (ref. 52). The measurements by Georgii indicate a surface mixing ratio of 1.5 to 3.0 ppb. This is close to the estimate of 0.2 ppb by Robinson and Robbins (ref. 31). Using this value as the lower boundary condition and zero flux at the tropopause, the model calculated the profile shown in figure 5. The model shows a very rapid decrease in the mixing ratio with altitude similar to Georgii's measurements.

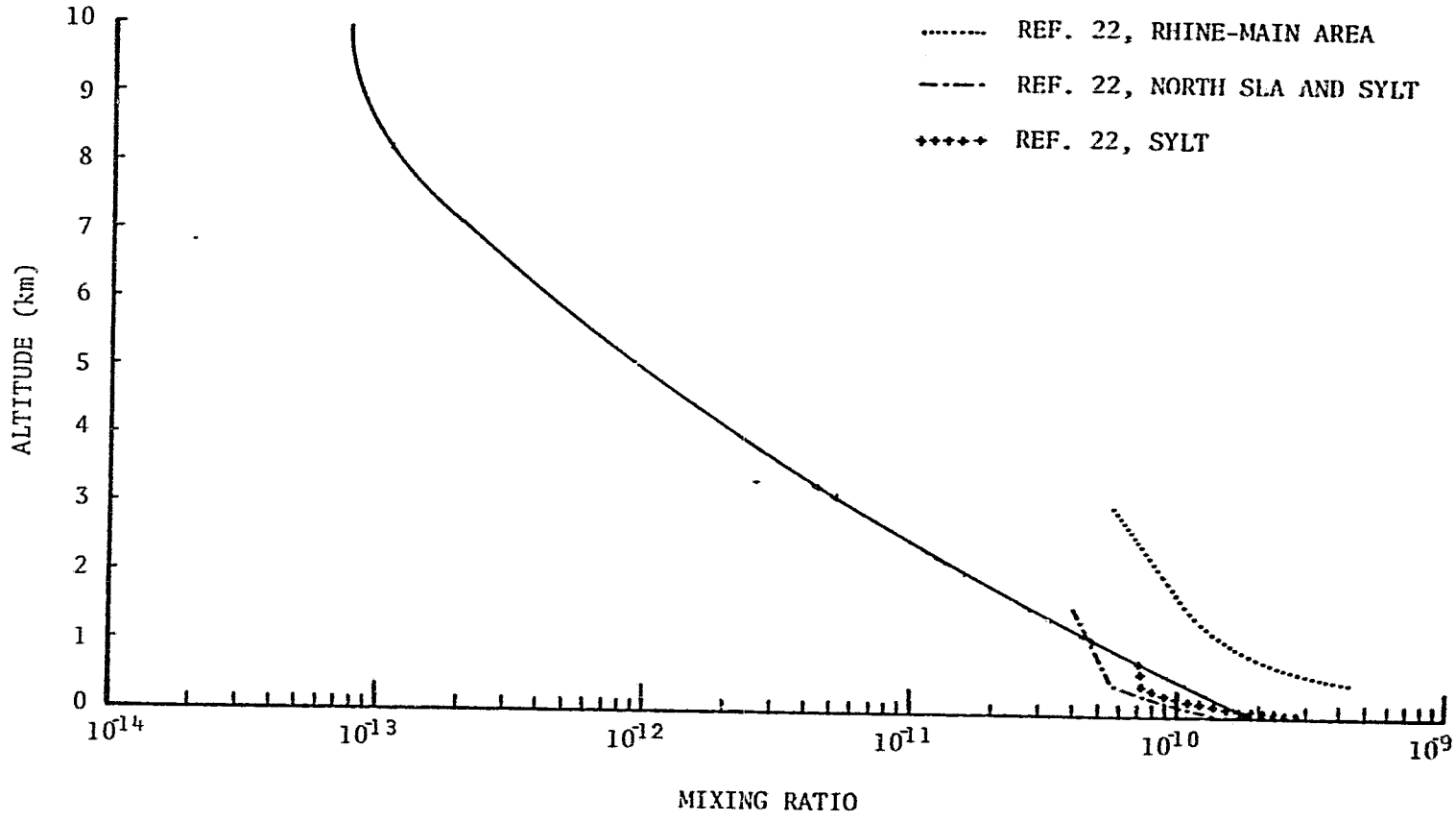

Figure 5. Calculated vertical profile of hydrogen sulfide (H_2S).

Carbon Disulfide (CS_2)

Chemical production.— No known chemical reaction in the atmosphere produces carbon disulfide.

Chemical loss.— The primary loss mechanism is the reaction with the hydroxyl radical, OH, (reaction 87). Minor loss contributions come from reactions with atomic oxygen (reactions 70, 71, and 72). The reaction of CS_2 to atomic sulfur, $S(^3p)$, (reaction 88) is negligible. The lifetime based on these reactions is slightly more than one month. This value compares reasonably well with the value of 0.2 years given by Sze and Ko (ref. 4).

Anthropogenic emission.— CS_2 is known to result from the manufacturing of petroleum (ref. 33) and of synthetic fiber (ref. 36).

Natural emission.— Carbon disulfide has been detected in the smoke from volcanoes (ref. 32). Also, some measurements in seawater (ref. 37) seem to indicate a natural source of CS_2.

Measurements of CS_2 are very sparse and confined to one location in England (ref. 23). The average surface value obtained was 0.19 ppb. No vertical measurements are available. Using the value of 0.19 ppb as the lower boundary condition and zero flux at the tropopause, the model calculated the profile shown in figure 6. CS_2 decreases relatively slowly with altitude, as would be expected from its moderately long lifetime.

Sulfuric Acid (H_2SO_4)

Chemical production.— Sulfuric acid is formed chemically by the reaction of sulfur trioxide, SO_3, with water vapor, H_2O, (reaction 80).

Chemical loss.— No gas phase chemical loss mechanism has yet been identified for H_2SO_4.

Anthropogenic emission.— Sulfuric acid has been detected in the exhaust of automobiles (ref. 36) and in the manufacturing process of H_2SO_4 (ref. 39).

Natural emission.— H_2SO_4 is present in volcanic emission (ref. 38).

Heterogeneous loss.— The only known loss mechanism for sulfuric acid is heterogeneous loss. In the NASA/LaRC model we used a heterogeneous loss rate similar to that of Turco et al. (ref. 5), again with the exception of a lower

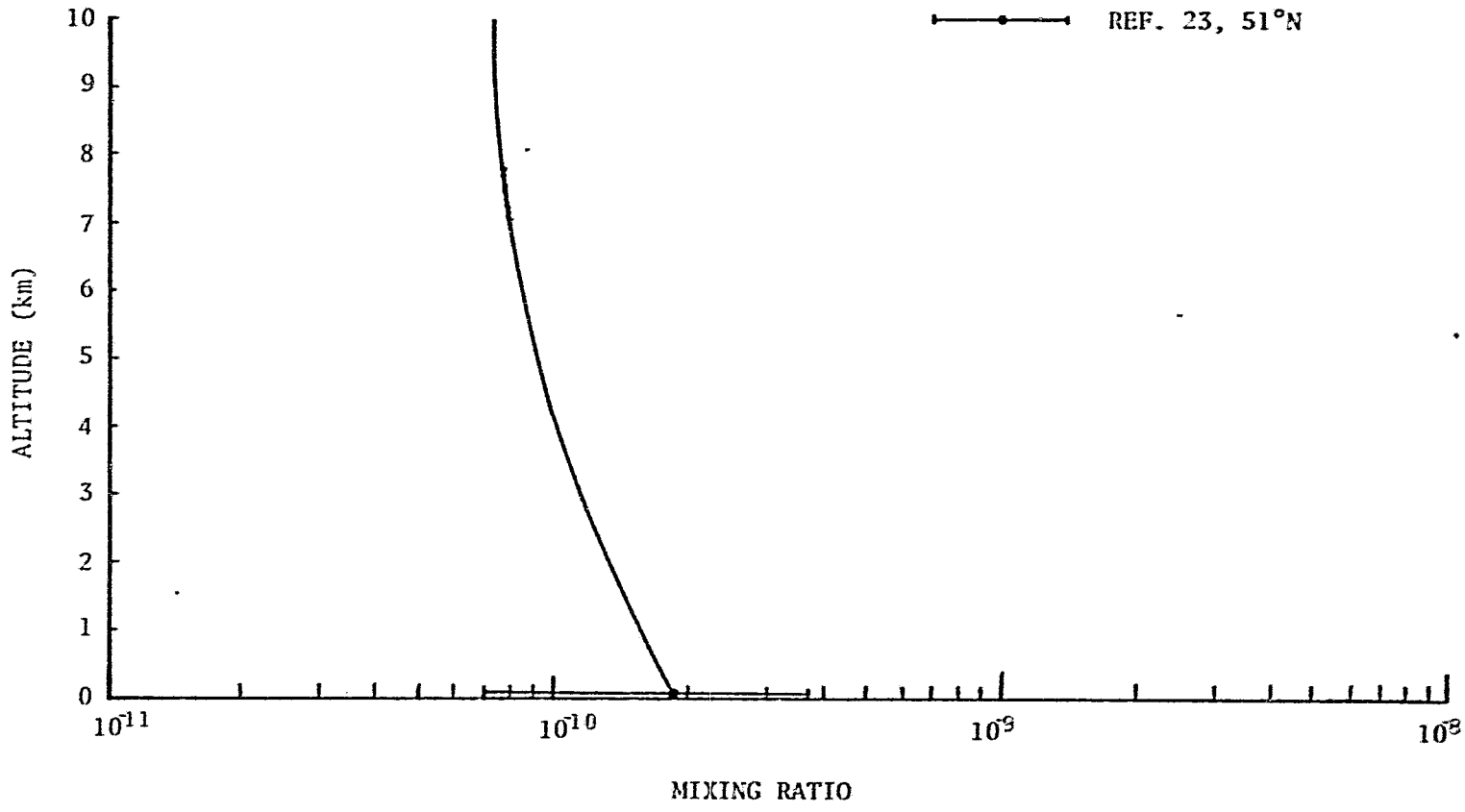

Figure 6. Calculated vertical profile of carbon disulfide (CS_2).

tropopause altitude (10 km vs. 13 km). The lifetime of H_2SO_4 at the surface based on this heterogeneous loss rate is about 0.5 day.

It is of utmost importance to learn the fate of the H_2SO_4 molecules. It can occur in liquid form and rainout in the form of acid rain which affects the environment adversely, or it can occur in solid form, which affects the growth of the aerosol layer and, hence, ultimately will affect the climate. In the model, a zero flux condition was imposed at both boundaries. The resulting vertical profile is shown in figure 7. There are no tropospheric measurements of H_2SO_4 for comparison.

Sulfurous Acid Radical (HSO_3)

Chemical production.— The only known chemical production is due to the reaction of SO_2 with OH (reaction 77).

Chemical loss.— Gas phase loss occurs as a result of the reaction of HSO_3 with OH (reaction 105). The homogeneous lifetime of HSO_3 is approximately 15 hours at the surface.

Anthropogenic and natural emission.— No anthropogenic or natural emissions are presently known.

Heterogeneous loss.— The heterogeneous loss term is modeled similar to H_2SO_4 (ref. 5). The combined lifetime due to both homogeneous and heterogeneous chemistry is about six hours at the surface.

It is of great interest to find out the details of the fate of the HSO_3 radical because it offers a loss mechanism for sulfur before oxidation to sulfuric acid occurs. As in the case of H_2SO_4, no atmospheric measurements of HSO_3 exist. The free acid H_2SO_3 is not believed to exist, while the bisulfates containing HSO_3 are well known (ref. 53). The boundary conditions chosen for HSO_3 are similar to those for H_2SO_4. The resulting profile is shown in figure 7. The profiles of HSO_3 and H_2SO_4 follow each other in shape very closely. This is due to the fact that the dominating heterogeneous loss term is identical for both molecules.

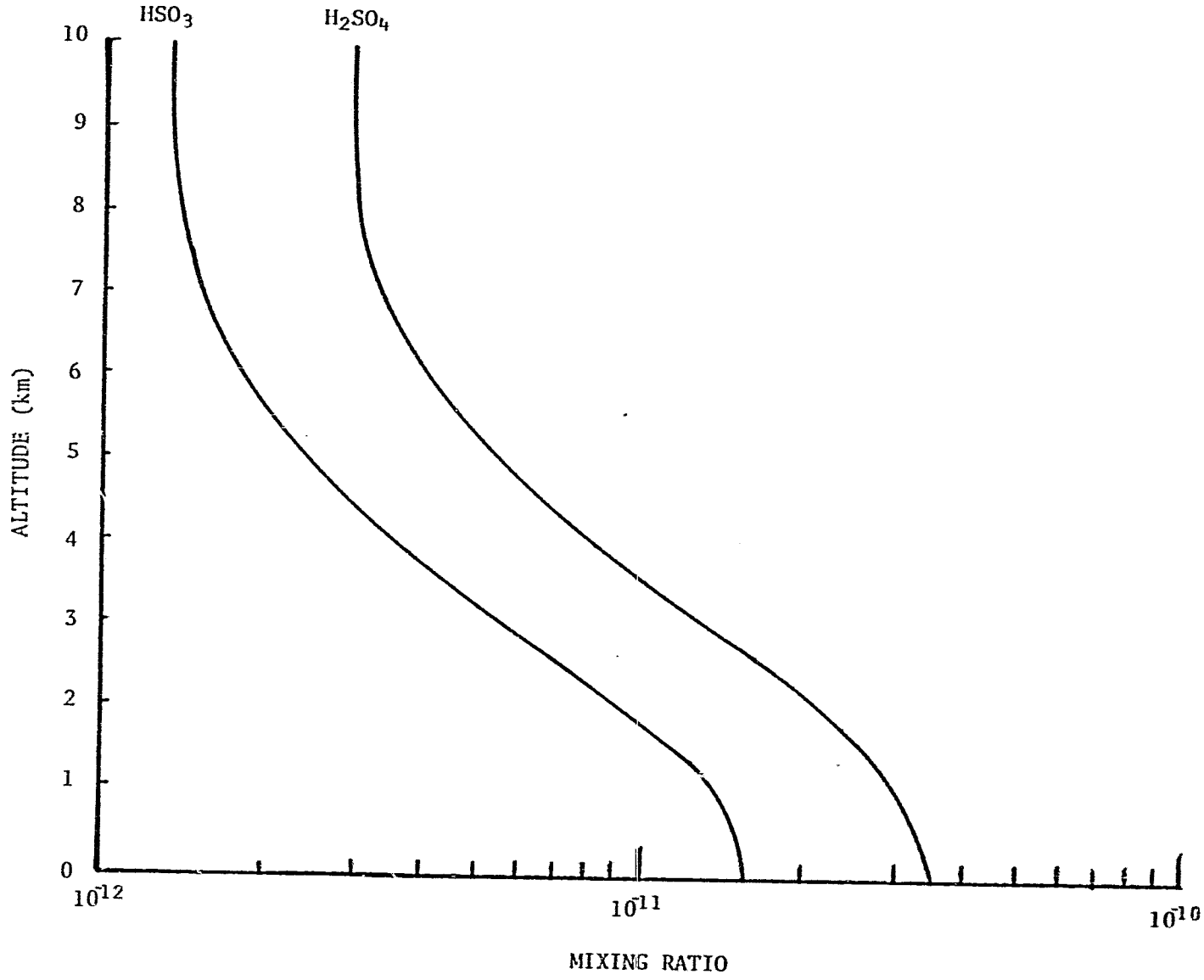

Figure 7. Calculated vertical profile of sulfuric acid (H_2SO_4) and of the sulfurous acid radical (HSO_3).

Intermediate Sulfur Species

Introduction.— The five short-lived intermediate sulfur species have only chemical production and loss mechanisms with the exception of sulfur trioxide, SO_3. Anthropogenic emissions of SO_3 have been detected in fuel-combustion processes (ref. 54) and in the manufacturing process of sulfuric acid (ref. 55). The following subsections will discuss the chemical production and loss mechanisms for each of the five intermediate species. Again, the chemcial reactions will be mentioned in order of importance.

Sulfoxy (SO).— SO is formed primarily by oxidation of the thiohydroxyl radical, HS, with molecular oxygen, O_2 (reaction 66). Of minor importance are the oxidations of carbon disulfide with O (reaction 70), carbon sulfide, CS, with O (reaction 74), atomic sulfur [$S(^3p)$] with O_2 (reaction 76) and carbonyl sulfide, COS, with O (reaction 101). The productions of SO due to the oxidations of the thiyl radical, HS, with O (reaction 65) and of sulfur dioxide, SO_2, with O (reaction 81) are negligible compared to the other reactions producing SO. Losses are due primarily to the oxidation of SO with O_2 (reaction 68). Minor losses are caused by the reaction of SO with NO_2 (reaction 69) and by SO reacting with ozone, O_3, (reaction 103). Negligible loss mechanisms include the reaction of SO with itself (reaction 90) and of SO reacting with SO_3 (reaction 91). Hence, the five loss mechanisms for SO nearly always produce SO_2. In only one instance, the reaction of SO with itself (reaction 90), is SO_2 not produced. Thus, SO acts as an important precursor to SO_2. The calculated lifetime of SO is on the order of 10^{-2} s. The vertical profile is plotted in figure 8. Due to its short lifetime and high reactivity, measurements cannot be made. This is true for the four remaining intermediate sulfur species also.

Carbon sulfide (CS).— CS is formed primarily when carbon disulfide is oxidized by atomic oxygen (reaction 70) and, of negligible importance, when atomic sulfur reacts with CS_2 (reaction 88). The two primary loss mechanisms are oxidation of CS with O_2 (reactions 74 and 75). The reaction of CS with O_2 takes two paths with equal preference. A negligible loss for CS is the oxidation with O (reaction 73). The lifetime of CS based on these reactions is on the order of 10^{-2} s, well justifying the PCE assumption. The vertical profile is shown in figure 8.

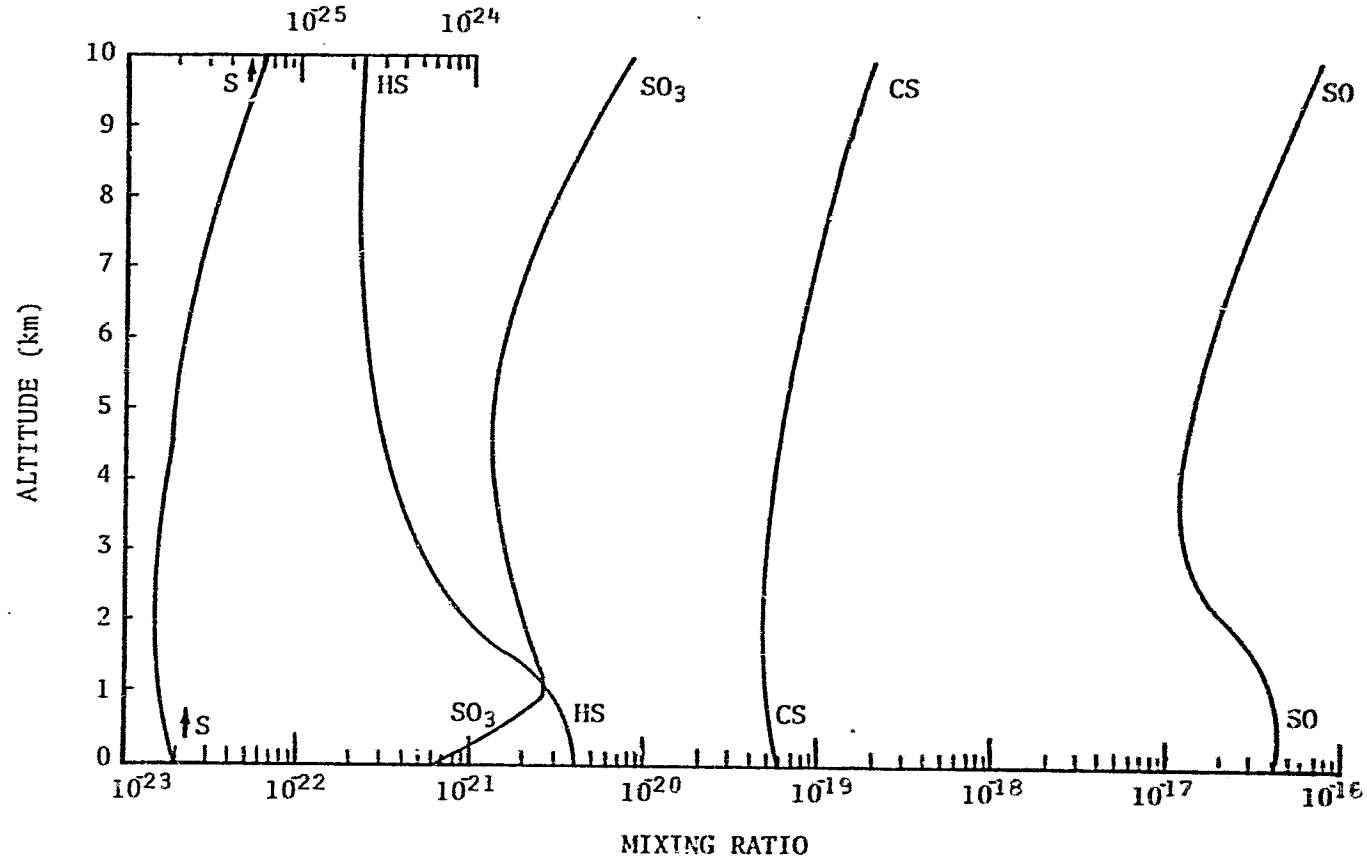

Figure 8. Calculated vertical profiels of the intermediate sulfur species. (Note the shifted scale for $S(^3p)$.)

Thiohydroxyl radical (HS).— The thiohydroxyl radical is a highly reactive species formed by seven reactions and destroyed by five. Three reactions are of importance for its formation: hydrogen sulfide reacting with the hydroxyl radical, OH, (reaction 64), carbon disulfide reacting with OH (reaction 87), and carbonyl sulfide reacting with OH (reaction 86). Minor production of HS is due to the oxidation of H_2S with O (reaction 102) and the reaction of H with H_2S (reaction 84). Of negligible importance are the reactions of COS with H (reaction 85) and S reacting with H_2 (reaction 83). Losses are due almost entirely to the oxidation of O_2 (reaction 66). Of negligible importance are the remaining four loss mechanisms: HS reacting with NO (reaction 67), HS oxidized by O (reaction 65), HS reacting with H (reaction 82), and HS reacting with itself (reaction 93). The resulting lifetime of the thiohydroxyl radical is very short, on the order of 10^{-6} s. Its calculated vertical profile is plotted in figure 8.

Sulfur trioxide (SO_3).— As mentioned previously, sulfur trioxide is the only intermediate sulfur species that has nonchemical production terms. The relative importance of chemical vs. nonchemical contributions to the total SO_3 budget is poorly understood. Chemically, SO_3 is produced primarily by the reaction of HSO_3 with OH (reaction 105) and by SO_2 reacting with the methylperoxy radical, CH_3O_2, (reaction 79). Minor contributors to SO_2 production are SO_2 reacting with HO_2 (reaction 78) and SO_2 being oxidized by O in the presence of a third body (reaction 104). The main path for SO_3 destruction is the reaction with water vapor, H_2O, (reaction 80). Of negligible importance is the reaction of SO_3 with SO (reaction 91). Sulfur trioxide is very short lived. Its lifetime is on the order of 10^{-6} s. The vertical profile due to the chemistry described above is plotted in figure 8.

Atomic sulfur [$S(^3p)$].— The production of atomic sulfur is due almost entirely to the reaction of CS_2 with O (reaction 71). Of negligible inportance are the four reactions: CS with O (reaction 73), SO with itself (reaction 90), HS reacting with H (reaction 83), and HS reacting with itself (reaction 93). Loss of S is primarily by oxidation with molecular oxygen (reaction 76). Minor contributors to loss of S are reactions with CS_2 (reaction 88) and with COS (reaction 89). The reaction of S with H_2 (reaction 83) is virtually negligible as a loss for atomic sulfur. The

lifetime of atomic sulfur is extremely short, about 10^{-7} s. The vertical profile of S is shown in figure 8. (Observe that the horizontal scale is shifted for S.)

FUTURE PERTURBATIONS TO THE SULFUR BUDGET

A couple of decades ago, the only global scale implication due to sulfur species was thought to be the formation of stratospheric particulates (ref. 2). This argument was based on the relatively moderate lifetimes of most sulfur species. Lifetimes on the order of a few days to a week were thought to preclude any real important contributions to global tropospheric chemistry. We now know that sulfur species play an integral part in the highly coupled and complex chemical system that constitutes the troposphere. SO_2 emissions had an upward trend during the 1960's. This trend was partially reversed during the 1970's. Some actions responsible for this decrease were a greater use of clean-burning natural gas and of crude oil with low sulfur content. Also, a slower economic growth coupled with energy conservation contributed to a decrease in SO_2 emissions. Recently, this trend has started upward again. The global concentrations of sulfur compounds are very likely to see a rapid increase in years to come due to energy policies. Already emission standards for many oil-burning power plants and industrial plants are relaxed to allow for usage of lower grade crude oil containing more sulfur. Anthropogenic emissions are currently responsible for approximately half as much of the atmospheric sulfur concentrations as are the natural emissions, but some 20 to 25 years from now manmade emissions may equal those of nature and may actually at the turn of the century surpass nature's emissions in the northern hemisphere (ref. 12). The estimates of global emission of sulfur are widely varying. Katz (ref. 49) made some early estimates and calculated that 77 Mt of SO_2 was emitted in 1943. The Study of Critical Environmental Problems (ref. 56) established a global emission of 93 Mt/yr in 1967 to 1968 Robinson and Robbins (ref. 31) estimated the annual total SO_2 emission in the mid-1960's to be 146 Mt. A more recent estimate (ref. 10) calculates the global manmade emissions of SO_2 to be 183 Mt. It is significant to note that of the total global emissions of SO_2, 93.5 percent occur in the northern hemisphere and only 6.5 percent in the southern hemisphere (ref. 56). The most recent estimate (ref. 10) of global

bacteriogenic production of SO_2 is 210 Mt. Fertilizers are thought to account for 33 Mt of the manmade emissions. This portion of the sulfur budget is very likely to increase further. In the SCEP report (ref. 56), some predictions for the future were made. An annual growth in fossile fuel usage of 4 percent between 1970 and 1980 was assumed, with a 3.5 percent growth rate from 1980 to 2000. By the year 2000 A.D., a global anthropogenic emission of 275 Mt/yr would occur (ref. 56). However, at the present time it seems that any prediction of future crude oil is risky at best.

It is very evident that future sulfur levels in the atmosphere are a strong function of man's activities. Many questions concerning sulfur species remain to be answered: for example, the exact amounts of naturally vs. anthropogenically produced sulfur need to be ascertained. Also, what is the global concentration of SO_2? Present measurements are too inconclusive and in part contradictory. Furthermore, short-term and long-term impacts of SO_2 emissions on the sulfur budget must be elucidated. The primary chemical loss for SO_2 is OH. The hydroxyl radical (OH) is very reactive and acts somewhat like a "tropospheric vacuum cleaner." In figure 9, the resulting SO_2 profiles due to a doubling of the current OH level and a decrease by 50 percent in the present OH level are plotted. Thus, any increase in the SO_2 level would compete with many other species for the OH radical. The budgets of these competing trace gases need to be addressed. The importance of homogeneous vs. heterogeneous loss for SO_2 needs further research. Presently, it is believed that 50 percent is lost homogeneously and 50 percent is lost heterogeneously, but this breakdown is a very crude estimate. The depositional velocity of SO_2 needs further pinpointing. Estimates vary from 0.1 to 2.5 cm s^{-1} with 1.0 cm s^{-1} as an average. The vertical profile of SO_2 is very dependent on this quantity, as already pointed out in figure 3. It is also urgent to find the mechanism that controls the SO_2 to sulfate (gas-to-particle) conversion. From figure 1 we can see that SO_2 is converted to H_2SO_4 via the intermediate species SO_3. A possible alternate reaction path involves the HSO_3 radical. The fate of this molecule is virtually unknown. Also, the kinetic data concerning the reactions that convert SO_2 to SO_4^{2-} need to be improved. Finally, the role of ammonia, NH_3, in aerosol formation needs to be addressed. NH_3 is

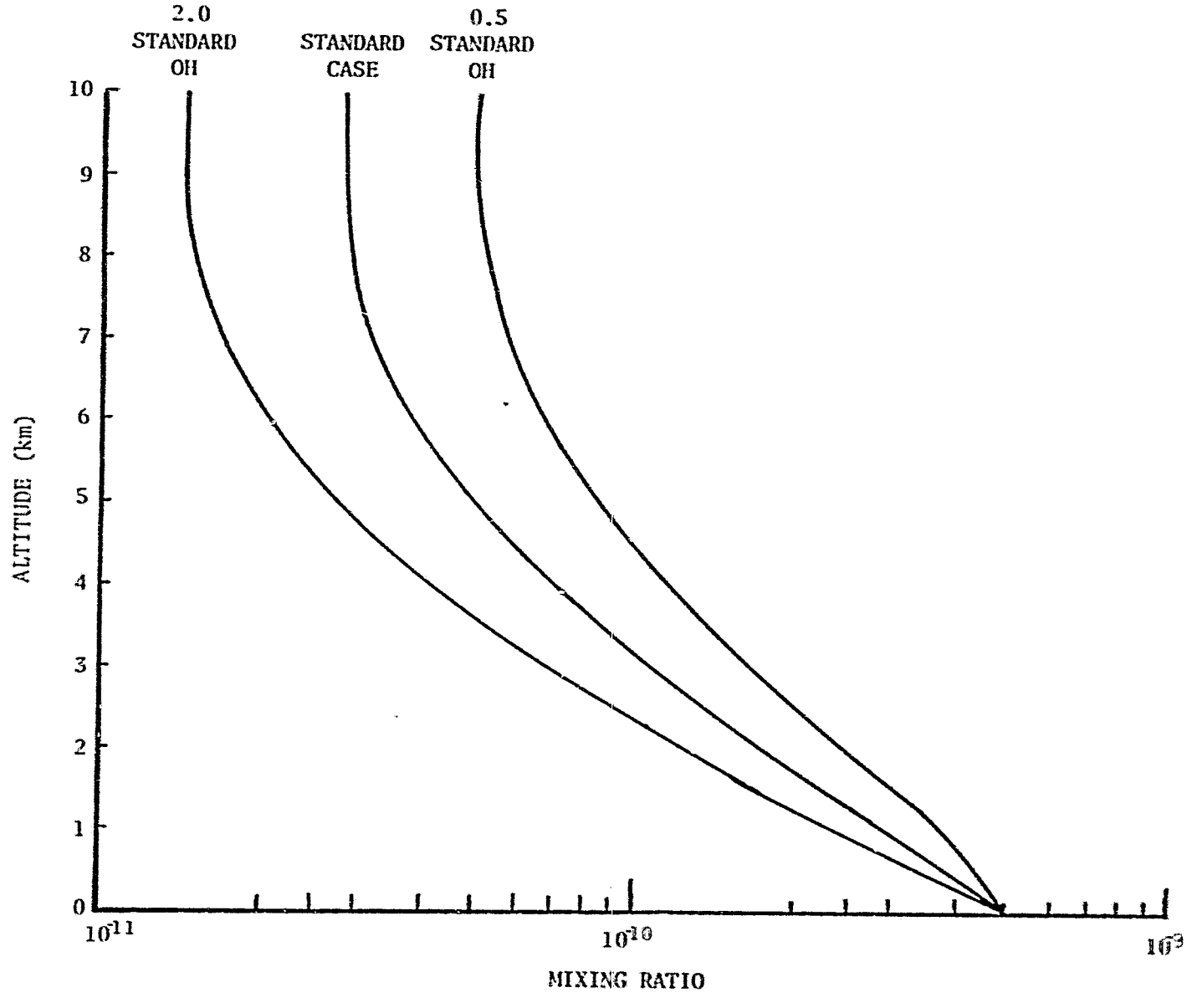

Figure 9. Vertical profiles of SO_2 as a function of varying the hydroxyl radical OH.

largely responsible for neutralizing the acidic sulfur species. Hence, if the sulfur budget increases more rapidly than the ammonia budget, an increase in acidic precipitation over the already high levels would result.

In conclusion, we have seen that the sulfur family, because it is largely so anthropogenic plays an increasingly important role in tropospheric chemistry. Additional research is needed to answer many of the questions related to the tropospheric sulfur budget. The answers to these questions will have a direct impact on many fields of scientific study, e.g., radiative transfer, climatology, meteorology, agronomy, ecology, and limnology, just to mention a few.

APPENDIX A

THE CONTINUITY EQUATION

The continuity equation can be written in either number density form or mixing ratio form. In the NASA/LaRC one-dimensional tropospheric photochemical model, the mixing ratio form is used. The vertical profile of a long-lived species is then expressed as:

$$\frac{\partial \phi_i}{\partial_z} = Q_i(n_j) - L_i(n_j)Mf_i \tag{A-1}$$

where ϕ_i is the vertical flux (molecules cm^{-2} s^{-1}) of the ith species, $Q_i(n_j)$ are the chemical production terms, and $L_i(n_j)Mf_i$ are the chemical loss terms of the ith species; M is the total number density (molecules cm^{-3}), f_i is the mixing ratio of the ith species, and M and f are related by the expression:

$$f_i = \frac{n_i}{M} \tag{A-2}$$

where n_i is the number density of the species under consideration. The vertical flux of the ith species, ϕ_i, can be written in terms of a parameterization, K_z:

$$\phi_i = -K_z \, M\left(\frac{\partial f_i}{\partial z}\right) \tag{A-3}$$

The term K_z is an empirical constant (cm^2 s^{-1}) usually called the eddy diffusion coefficient. The word "eddy" is somewhat of a misnomer since it indicates that the diffusive process occurs on a small scale. On the contrary, most vertical transport in the troposphere takes place on a very large scale. Substitution of equation (A-3) into equation (A-1) yields:

$$\frac{\partial}{\partial z}\left[K_z \, M\left(\frac{\partial f_i}{\partial z}\right)\right] = -Q_i(n_j) + L_i(n_j) \, Mf_i \tag{A-4}$$

Because equation (A-4) usually depends on many species other than the ith, it is a highly coupled, nonlinear, partial differential equation that has to be solved numerically.

In the case of short-lived species, the chemistry dominates the vertical distribution. For these species the vertical transport terms [i.e. the terms on the left-hand side of equation (A-4)] can be neglected. This condition is known as photochemical equilibrium (PCE). If the PCE assumption is justified, the solution of equation (A-4) is simplified considerably since we can solve explicitly for f_i:

$$f_i = \frac{Q_i(n_j)}{L_i(n_j)M} \tag{A-5}$$

Hence, in the cases where PCE can be used, a high degree of computational efficiency, both in terms of time and money, can be reached.

APPENDIX B

NUMERICAL SOLUTION OF THE CONTINUITY EQUATION

The NASA/LaRC one-dimensional, global, tropospheric, photochemical model calculates the continuity equation in the mixing ratio form, previously given in equation (A-4):

$$\frac{\partial}{\partial z}\left[K_z\ M\left(\frac{\partial f_i}{\partial z}\right)\right] = -Q_i(n_j) + L_i(n_j)\ Mf_i \tag{B-1}$$

By expanding on the derivative with respect to altitude and rearranging the terms in equation (B-1) we obtain:

$$K_z\ M\ \frac{\partial^2 f_i}{\partial z^2} + \frac{\partial}{\partial z}\ (K_z\ M)\ \frac{\partial f_i}{\partial z} - L_i(n_j)\ Mf_i + Q_i(n_j) = 0 \tag{B-2}$$

After dividing this equation by M we obtain:

$$K_z\ \frac{\partial^2 f_i}{\partial z^2} + \frac{1}{M}\frac{\partial}{\partial z}\ (K_z\ M)\ \frac{\partial f_i}{\partial z} - L_i(n_j) f_i + \frac{Q_i(n_j)}{M} = 0 \tag{B-3}$$

Equation (B-3) defines a system of equations for each species, f_i. A finite-difference scheme is used to solve the equations (ref. 57). The finite-difference equations are defined as:

$$\frac{\partial^2 f}{\partial z^2} \rightarrow \frac{f_{k+1} - {}^2f_k + f_{k-1}}{\Delta z^2} \text{ (for second order equations)} \tag{B-4}$$

and

$$\frac{\partial f}{\partial z} \rightarrow \frac{f_{k+1} - f_{k-1}}{2\Delta z} \text{ (for first order equations)} \tag{B-5}$$

Substituting these equations into equation (B-3), rearranging terms and dropping the species index i and subscript z on K_z, we obtain:

$$f_{k+1}\left[\frac{K_k}{\Delta z^2} + \frac{A}{2\Delta z}\right] + f_k\left[-\frac{2K_k}{\Delta z^2} - L\right] + f_{k-1}\left[\frac{K_k}{\Delta z^2} - \frac{A}{2\Delta z}\right] = \frac{Q}{M} \qquad \text{(B-6)}$$

The term A represents: $\frac{1}{M}\frac{\partial(K_z\ M)}{\partial z}$, and the index k refers to the spatial derivative z. Equation (B-6) can be written in finite-difference form as:

$$\vec{A} \cdot f_{k+1} + \vec{B} \cdot f_k + \vec{C} \cdot f_{k-1} = \vec{D} \qquad \text{(B-7)}$$

APPENDIX C

BOUNDARY CONDITIONS

Two types of boundary conditions are available to solve the continuity equation. We can either specify a mixing ratio f_i or a flux ϕ_i, upward or downward at the upper and lower boundaries. In general, the boundary condition can be written as:

$$a_i \cdot \frac{\partial f_i}{\partial z} + b_i \cdot f_i = c_i \tag{C-1}$$

If we specify a mixing ratio f_i at the lower boundary, $a_i = 0$, $b_i = 1$, and equation (C-1) becomes:

$$f_i = c_i \tag{C-2}$$

or, in finite-difference form:

$$\vec{B}_\ell \cdot f_\ell = \vec{D}_\ell \tag{C-3}$$

where the subscript ℓ is used to denote lower boundary. If a mixing ratio is specified at the upper boundary, $a_i = 1$, $b_i = 0$, and equation (C-1) becomes

$$a_i \cdot \frac{\partial f_i}{\partial z} = c_i \tag{C-4}$$

In finite-difference form (with subscript u for upper boundary):

$$\vec{B}_u \cdot f_u + \vec{C}_u \cdot f_u = \vec{D}_u \tag{C-5}$$

This result is obtained from an expansion of equation (C-4):

$$\frac{f_u - f_{u-1}}{\Delta z} = c_u \tag{C-6}$$

This can be rearranged to:

$$f_u - f_{u-1} = c_u \, \Delta z \tag{C-7}$$

which in finite-difference form can be written as equation (C-5), with $\vec{B}_u = 1$, $\vec{C}_u = 0$, and $\vec{D}_u = c_u \, \Delta z$.

For an upward or downward flux across the upper boundary, the boundary condition reduces to:

$$\frac{\partial f(\phi)_u}{\partial z} = c(\phi)_u \tag{C-8}$$

The finite-difference form looks similar to equation (C-5):

$$\vec{B}(\phi)_u \cdot f(\phi)_u + \vec{C}(\phi)_u \cdot f(\phi)_u = \vec{D}(\phi)_u \tag{C-9}$$

In this case, $\vec{B}(\phi)_u = 1$, $\vec{C}(\phi)_u = -1$, $\vec{D}(\phi)_u = C(\phi)_u = C(\phi)_u \, \Delta z$, and $\vec{A}(\phi)_u = 0$. For a flux, upward or downward, across the lower boundary, equations (C-8) and (C-9) are still valid, except in this case $\vec{B}(\phi)_\ell = -1$, $\vec{C}(\phi)_\ell = 1$, $\vec{D}(\phi)_\ell = C(\phi)_\ell \, \Delta z$, and $A(\phi)_\ell = 0$.

Equation (B-7) from Appendix B, together with equations (C-3) and (C-5), forms a so-called "block tridiagonal" system of equations given by:

$$
\begin{bmatrix}
\vec{B} & \vec{A}_{\ell} & 0 & . & . & . & . & . & 0 \\
\vec{C}_2 & \vec{B}_2 & \vec{A}_2 & 0 & . & . & . & . & 0 \\
0 & \vec{C}_3 & \vec{B}_3 & \vec{A}_3 & . & . & . & . & 0 \\
. & . & . & . & . & . & . & . & . \\
0 & . & . & 0 & \vec{C}_{u-1} & \vec{B}_{u-1} & & & \vec{A}_{u-1} \\
0 & . & . & . & 0 & \vec{C}_u & & & \vec{B}_u
\end{bmatrix}
\begin{bmatrix}
f_{\ell} \\ f_2 \\ f_3 \\ . \\ f_{u-1} \\ f_u
\end{bmatrix}
=
\begin{bmatrix}
\vec{D}_{\ell} \\ \vec{D}_2 \\ \vec{D}_3 \\ . \\ \vec{D}_{u-1} \\ \vec{D}_u
\end{bmatrix}
\qquad \text{(C-10)}
$$

There are several numerical techniques available to solve the tridiagonal matrix described by equation (C-10). In the NASA/LaRC model, a Gaussian elimination method without pivoting is used (ref. 57).

APPENDIX D

PHOTODISSOCIATION RATE CALCULATIONS

In order to calculate the photodissociation rates, one first must determine the amount of incoming solar radiation. The incident radiation is a function of wavelength λ, altitude z, and solar zenith angle θ [i.e., $I = I(\lambda,z,\theta)$]. The expression for incident solar radiation is due to Leighton (ref. 58):

$$I(\lambda,z,\theta) = I_o(\lambda)*\exp[-\tau_{O_3}(\lambda)\sec\theta] * \left\{\exp[-\tau_p(\lambda) - \tau_r(\lambda)]\sec\theta + \left[1 - \exp[-\tau_p(\lambda) - \tau_r(\lambda)]\sec\theta\right]\cos\theta\right\} \quad \text{(D-1)}$$

where $I_o(\lambda)$ is the incident solar flux at the top of the atmosphere. This has been tabulated by Ackerman (ref. 59). The term $\exp[-\tau_{O_3}(\lambda) \cdot \sec\theta]$ is the attenuation due to ozone absorption. The next term $\exp[-\tau_p(\lambda) - \tau_r(\lambda)]\sec\theta$ is the direct solar attenuation due to aerosol particle scattering (τ_p) and Rayleigh scattering (τ_r). The last term $[1 - \exp[-\tau_p(\lambda) - \tau_r(\lambda)\sec\theta]\cos\theta$ is the diffuse solar radiation attenuated by aerosol and Rayleigh scattering. Values for $\tau_p(\lambda)$ and $\tau_r(\lambda)$ have been tabulated by Elterman (ref. 60). Once the incident solar radiation, $I(\lambda,z,\theta)$ is known, the photodissociation rates, J_i, can be calculated according to:

$$J_i(\lambda,z,\theta) = \sum_{\lambda=1}^{n} \Delta I_j(\lambda,z,\theta)\sigma_i(\lambda) \quad \text{(D-2)}$$

where $\sigma_i(\lambda)$ is the molecular cross section of the ith species. The solar zenith angle, θ, is calculated as:

$$\cos\theta = \cos\phi * \cos\delta * \cos t + \sin\phi * \sin\delta, \quad \text{(D-3)}$$

where ϕ is the latitude, δ is the solar declination angle and t is the local hour angle of the sun. For a given latitude (ϕ) and solar declination (δ), the local hour angle of the sun (t) varies from -180°

to 180° with each hour corresponding to a 15° increment, i.e., local noon is 0°, 11 a.m. is -15°, 1 p.m. is +15°, etc.

APPENDIX E

CONVERGENCE CRITERIA

The model imposes two separate convergence criteria, one for the species in photochemical equilibrium and one for the species that are calculated using the continuity equation. The number of iterations needed is a strong function of the initial profiles that are prescribed. In general, the flow of the calculations of the model is as follows: First, the initial profiles for all species are prescribed. Secondly, the reaction rate constants are calculated. Next, the incident solar radiation is calculated, and based on these results, the photodissociation rates are computed. The model then calculates the vertical profiles of the short-lived species in photochemical equilibrium. Finally, the long-lived species that are transported are calculated. The vertical profiles that are obtained for the species are compared to the previous iteration and recalculated until the convergence criteria is achieved. For the short-lived species, the convergence criteria is

$$\left| 1 - \frac{(n_i)_1}{(n_i)_2} \right| < 10^{-6} \qquad \text{(E-1)}$$

and for the transported species the criteria is

$$\left| 1 - \frac{(n_i)_1}{(n_i)_2} \right| < 10^{-4} \qquad \text{(E-2)}$$

Computationally, the photochemical equilibrium species are calculated much more rapidly than the transported species; therefore, a somewhat more stringent convergence criteria can be imposed on the PCE species. With reasonably close initial guesses of the vertical profiles (i.e., vertical profiles within a couple of orders of magnitude of the final profiles), convergence is achieved after three to four iterations for the short-lived species and five to six iterations for the long-lived species.

REFERENCES

1. Crutzen, P.J.: The Possible Importance of CSO for the Sulfate Layer of the Stratosphere. Geophys. Res. Lett., Vol. 3, 1976, pp. 73-76.

2. Junge, C.E.; Chagnon, C.W.; and Manson, J.E.: Stratospheric Aerosols. J. Meteor., Vol. 18, 1961, pp. 81-108.

3. Junge, C.E.: Proc. IAMAP Conf. on Structure, Composition and General Circulation of Upper and Lower Atmos., 1974, pp. 85-97.

4. Sze, N.D.; and Ko, M.K.W.: CS_2 and COS in the Stratospheric Sulfur Budget, Nature, Vol. 280, 1979, pp. 308-310.

5. Turco, R.P.; Hamill, P.; Toon, O.B.; Whitten, R.C.; and Kiang, C.S.: A One-Dimensional Model Describing Aerosol Formation and Evolution in the Stratosphere: I. Physical Processes and Mathematical Analogs. J. Atmos. Sci., Vol. 36, 1979, pp. 699-717.

6. Logan, J.A.; McElroy, M.B.; Wofsy, S.C.; and Prather, M.J.: Oxidation of CS_2 and COS: Sources for Atmospheric SO_2. Nature, Vol. 281, 1979, pp. 185-188.

7. Likens, G.E.: Acid Precipitation. Chem. & Eng. News, Vol. 54, No. 48, 1976, pp. 29-44.

8. Mizutani, H. et al.: Odor Pollution Research in Nagoya City, Taiki Osen Kenkyu, Vol. 8, 1973, p. 381.

9. Shaw, R.W.: Acid Precipitation in Atlantic Canada. Environ. Sci. & Tech., Vol. 13, 1979, pp. 406-411.

10. Shinn, J.H.; and Lynn, S.: Do Man-Made Sources Affect the Sulfur Cycle of Northeastern States? Environ. Sci. and Tech., Vol. 13, 1979, pp. 1062-1067.

11. Levine, J.S.; and Schryer, D.R., eds.: Man's Impact on the Troposphere. Lectures in Tropospheric Chemistry. NASA Reference Publication 1022, 1978, pp. 27-64.

12. Kellogg, W.W.; Cadle, R.D.; Allen, E.R.; Lazrus, A.L.; and Martell, E.A.: The Sulfur Cycle. Science, Vol. 175, No. 4022, 1972, pp. 587-596.

13. Augustsson, T.R.; Levine, J.S.; and Tiwari, S.N.: The Sulfur Budget of the Troposphere. EOS, Vol. 61, No. 17, 1980, p. 239.

14. Levine, J.S.; Augustsson, T.R.; and Hoell, J.M.: The Vertical Distribution of Atmospheric Ammonia. Geophys. Res. Lett., Vol. 7, 1980, pp. 317-320.

15. Levine, J.S.; Augustsson, T.R.; and Hoell, J.M.: The Ammonia Budget of the Atmosphere/Biosphere System. EOS, Vol. 61, No. 17, 1980, p. 239.

16. Hoell, J.M.; Harward, C.N.; and Williams, T.S.: Remote Infrared Heterodyne Radiometer Measurements of Atmospheric Ammonia Profiles, Geophys. Res. Lett., Vol. 7, 1980, pp. 313-316.

17. Hoell, J.M.; Levine, J.S.; Augustsson, T.R.; and Harward, C.N.: Atmospheric Ammonia: Measurements and Modeling. AIAA Paper 81-0376, Jan. 1981.

18. Augustsson, T.R.; Levine, J.S.; and Tiwari, S.N.: The Effect of Isotropic Multiple Scattering and Surface Albedo on the Photochemistry of the Troposphere. EOS, Vol. 61, No. 46, 1980, p. 966.

19. Wang, W.C.; Yung, Y.L.; Lacis, A.A.; Mo, T.; and Hansen J.E.: Greenhouse Effects Due to Man-Made Perturbations of Trace Gases. Science, Vol. 194, 1976, pp. 685-690.

20. Georgii, H.W.; and Gravenhorst, G.: The Ocean as Source or Sink of Reactive Trace-Gases. PAGEOPH, Vol. 115, 1977, pp. 503-511.

21. Maroulis, P.J.; Goldberg, A.B.; and Bandy A.R.: Measurements of Tropospheric Background Levels of SO_2 on Project GAMETAG. Trans. Am. Geophys. Un., Vol. 59, 1978, pp. 1081-1082.

22. Georgii, H.W.: Large Scale Spatial and Temporal Distribution of Sulfur Compounds. Atmos. Environ., Vol. 12, 1978, pp. 681-690.

23. Sandalls, F.J.; and Penkett, S.A.: Measurements of Carbonyl Sulfide and Carbon Disulfide in the Atmosphere. Atmos. Environ., Vol. 11, 1977, pp. 197-199.

24. Maroulis, P.J.; Torres, A.L.; and Bandy, A.R.: Atmospheric Concentrations of Carbonyl Sulfide in the Southwestern and Eastern United States. Geophys. Res. Lett., Vol 4, 1977, pp. 510-512.

25. Torres, A.L.; Maroulis, P.J.; Goldberg, A.B.; and Bandy, A.R.: Measurements of Tropospheric OCS on the 1978 GAMETAG Flights. Trans. Am. Geophys. Un., Vol 59, 1978, p. 1082.

26. Hanst, P.L.; Speller, L.L.; Watts, D.M.; Spence, J.W.; and Miller, M.F.: Infrared Measurements of Fluorocarbons, Carbon Tetrachloride, Carbonyl Sulfide, and Other Atmospheric Trace Gases. J. Air Pollut. Contr. Assoc., Vol. 25, 1975, pp. 1220-1226.

27. Schlegel, H.G.: Production, Modification, and Consumption of Atmospheric Trace Gases by Micro-organisms. Tellus, Vol. 26, 1974, pp. 11-20.

28. Huntington, A.T.: The Collection and Analysis of Volcanic Gases from Mount Etna. Phil. Trans. Roy. Soc. London, Ser. A, Vol, 274, 1973, pp. 119-128.

29. Bethge, P.O.; and Ehrenborg, L.: Identification of Volatile Compounds in Kraft Mill Emissions. Sv. Papperstidn., Vol. 70, 1967, pp. 347-350.

30. Kaijo, T.; Tsujimoto, T.; And Takahaski, T.: Odor Pollution of Kashima District. Taiki Osen Kenkya, Vol. 6, 1971, p. 222.

31. Robinson, E.; and Robbins, R.C.: Sources, abundances, and fate of gaseous atmospheric pollutants. SRI Project PR-6755, Stanford Res. Inst., 1968.

32. Stoiber, R.E.; and Jepsen, A.: Sulfur Dioxide Concentrations to the Atmosphere by Volcanoes. Science, Vol. 182, 1973, pp. 577-578.

33. Tsifrinovich, A.N.; Lulova, N.I.: Composition of Organo-sulfur Trace Impurities in Gases. Neftepererab. Neftekhim. Moscow, Vol. 6, 1972, pp. 33-35.

34. Environmental Protection Agency, Air Quality Criteria for Sulfur Oxides, Rep. AP-50 (Washington, DC), 1969, pp. 19-20.

35. Environmental Protection Agency, Air Quality Data — 1973 Annual Statistics, Rep. EPA-450/2-74-015, (Research Triangle Park, NC), 1974, pp. 69-112.

36. Environmental Protection Agency, Air Pollution Emission Factors, Rep. AP-42 (Research Triangle Park, NC), 1973-1975.

37. Lovelock, J.E.: CS_2 and the Natural Sulfur Cycle. Nature, Vol. 248, 1974, pp. 625-626.

38. Cadle, R.D. et al.: Trace Constituents Emitted to the Atmosphere by Hawaiian Volcanoes, Chemosphere, Vol. 2, 1973, pp. 231-234.

39. Challis, E.J.: The Approach of Industry to the Assessment of Environmental Hazards. Proc. Roy. Soc., Ser. B, Vol. 185, 1974, pp. 183-197.

40. Dickson, W.: Report No. 54, Institude of Freshwater Research (Drottingholm, Sweden), 1975, p. 8.

41. Davis, D.D.; Smith, G.; and Klauber, G.: Trace Gas Analysis of Power Plant Plumes via Aircraft Measurements: O_3, NO_x and SO_2 Chemistry. Science, Vol. 186, 1974, pp. 733-736.

42. Davis, D,D,; and Klauber, G.: Atmospheric Gas Phase Oxidation Mechanisms for the Molecule SO_2. Int. J. Chem. Kin. Symp., Vol. 1, 1975, pp. 543-556.

43. Graedel, T.E.: Sulfur Dioxide, Sulfate Aerosol and Urban Aerosol. Geophys. Res. Lett., Vol. 3, 1976, pp. 181-184.

44. Fujii, T. et al.: Studies on the Air Pollution by Exhaust Gases of Aircraft (1). Taiki Osen Kenkyu, Vol. 8, 1975, p. 515.

45. Jost, D.: Aerological Studies on the Atmospheric Sulfur-Budget. Tellus, Vol, 26, 1974, pp. 206-213.

46. Jaeschke, W.; Schmitt, R.; and Georgii, H.W.: Preliminary Results of Stratospheric SO_2-Measurements. Geophys. Res. Lett., Vol. 3, 1976, pp. 517-519.

47. Garland, J.A.: Atmos. Environ., Vol. 12, 1978, pp. 349-362.

48. Hicks, B.B.; Liss, P.S.: Tellus, Vol. 28, 1976, pp. 349-354.

49. Katz, M.: In : Air Pollution Handbook, P.L. Magill, F.R. Holden, and C. Ackley, eds. McGraw-Hill (N.Y.), 1956, pp. 2-1 to 2-56.

50. Tsuji, M.; and Okuno, T.: The GC Analysis of Carbonyl Sulfide Emitted by the Viscose Plant. In : Proceedings of the 13th Symposium of the Japan Society of Air Pollution (Tokyo), 1972, p. 119.

51. Hartstein, A.M.; and Forshey, D.R.: Coal Mine Combustion Products: Neoprenes, Polyvinyl Chloride Compositions, Urethane Foam, and Wood. U.S. Bur. Mines Rep. Invest., Vol. 7977, No. 15, 1974.

52. Slatt, B.J.; Natusch, D.F.S.; Prospero, J.M.; and Savoie, D.L.: Atmos. Environ., Vol. 12, 1978, pp. 981-991.

53. Cotton, F.A.; and Wilkenson G.: Advanced Inorganic Chemistry, John Wiley & Sons (N.Y.), 1966.

54. Chass, R.L.; and George, R.E.: Contaminant Emissions from the Combustion of Fuels. J. Air Pollut. Contr. Assoc., Vol. 10, 1960, pp. 34-43.

55. Heller, A.N.; Cuffe, S.T.; and Goodwin, D.R.: Inorganic Chemical Industry. In : Air Pollution, 2nd Ed., Vol. III, A.C. Stern, ed., Academic Press (N.Y.), 1968, pp. 191-242.

56. Man's Impact on the Global Environment. Report of the Study of Critical Environmental Problems (SCEP). MIT Press (Cambridge, Mass.), 1970.

57. Smith, G.D.: Numerical Solution of Partial Differential Equations. Oxford Univ. Press (London), 1965.

58. Leighton, P.A.: Photochemistry of Air Pollution. Academic Press (N.Y.), 1961, 300 pp.

59. Ackerman, M.: Ultraviolet Solar Radiation Related to Mesopheric Processes. Inst. Aeron. Spatiale Belg. Brussels, Vol. A-77, 1970, pp. 149-150.

60. Elterman, L.: UV, Visible, and IR Attenuations for Altitudes to 50 km. Environ. Res. Pap. 285. U.S. Air Force Cambridge Research Laboratory (Bedford, Mass.), 1968, pp. 1-48.